

Statistical mechanics of the maximum-average submatrix problem

Vittorio Erba¹, Florent Krzakala², Rodrigo Pérez², and Lenka Zdeborová¹

¹*Statistical Physics of Computation Laboratory,*

²*Information, Learning and Physics Laboratory,*

École polytechnique fédérale de Lausanne (EPFL) CH-1015 Lausanne

(Dated: March 10, 2023)

We study the maximum-average submatrix problem, in which given an $N \times N$ matrix J one needs to find the $k \times k$ submatrix with the largest average of entries. We study the problem for random matrices J whose entries are i.i.d. random variables by mapping it to a variant of the Sherrington-Kirkpatrick spin-glass model at fixed magnetization. We characterize analytically the phase diagram of the model as a function of the submatrix average and the size of the submatrix k in the limit $N \rightarrow \infty$. We consider submatrices of size $k = mN$ with $0 < m < 1$. We find a rich phase diagram, including dynamical, static one-step replica symmetry breaking and full-step replica symmetry breaking. In the limit of $m \rightarrow 0$, we find a simpler phase diagram featuring a frozen 1-RSB phase, where the Gibbs measure is composed of exponentially many pure states each with zero entropy.

We consider the maximum-average submatrix (MAS) problem, i.e. the problem of finding the $k \times k$ submatrix of an $N \times N$ matrix J with the largest average of entries. This is a natural combinatorial optimization problem that has been studied in the mathematical and data science literature [1], mainly in the context of biclustering [2]. Theoretical works focused on the case where J is a random matrix (*i.i.d.* standard Gaussian entries), the size of J is large ($N \rightarrow \infty$) and the size of the submatrix $k \ll N$ [3–5].

From a statistical physics point of view, the MAS problem is a natural variant of the well-known Sherrington-Kirkpatrick model [6] with spins $\sigma_i \in \{0, 1\}$ at fixed magnetization. Statistical physics of disordered systems and the related replica method have been used widely to study other combinatorial optimization problems such as graph partitioning [7], matching [8], graph colouring [9], K -satisfiability of Boolean formulas [10], and many others. As far as we are aware, the maximum-average submatrix problem has not been studied from the statistical physics point of view. Filling this gap is the main purpose of the present paper.

Our results reveal the phase diagram of the MAS problem when $k = mN$, N is large and m finite. We unveil that at large values of m as the submatrix average increases the system undergoes a continuous phase transition to a full replica symmetry breaking (RSB) phase [11]. At intermediate values of m the phase transition becomes discontinuous, passing through a dynamical one-step RSB and static one-step RSB phases to a full-RSB one [11]. At yet lower m , the full-RSB phase then vanishes and the maximum average is given by the one-step RSB solution. In the limit of $m \rightarrow 0$, the MAS problem behaves in a way related to the random energy model [12] presenting frozen one-step RSB [13, 14].

We also find that in the limit $m \rightarrow 0$ the phase diagram presents a region where polynomial algorithms are proven to work [4] yet according to our results the equilibrium behaviour of the problem is given by the frozen one-step RSB phase that is considered algorithmically hard [15].

One other such problem is known in the literature – the binary perceptron. For the binary perceptron, an explanation of the discrepancy between equilibrium properties and algorithmic feasibility has been proposed in relation to out-of-equilibrium large-local-entropy regions of the phase space that are not described within the standard replica solution [16]. This finding has been used to discuss learning in artificial neural networks [17] and to propose new algorithms [18]. The analogy of behaviour between the binary perceptron and the MAS problem is therefore interesting as it may serve to shed more light on the fundamental question of algorithmic hardness. From the point of view of the mathematics of spin glasses, the perceptron problem is difficult to handle due to the effective bipartite structure of the correlations. The MAS problem belongs instead to a class of problems for which the exactness of the replica calculation has been established rigorously in [19].

We now review the mathematical results which we later connect to our analysis. All these results hold in the regime $k \ll N$. In [3], the authors proved that the globally optimal submatrix has an average equal to $A_{\text{opt}} = 2\sqrt{\log N/k}$. They also conjectured, and it was later proven by [4], that the Largest Average Submatrix (\mathcal{LAS}) algorithm — an efficient iterative row/column optimization scheme — fails to reach the global optimum, as its fixed point — akin to local minima — has with high probability average equal to $A_{\mathcal{LAS}} = \sqrt{2\log N/k}$. The fact that the \mathcal{LAS} algorithm fails bears a natural question: is $A_{\mathcal{LAS}}$ an algorithmic threshold signalling the onset of a hard phase? In [4], the authors introduced a new algorithm called Incremental Greedy Procedure (\mathcal{IGP}) which is able to produce submatrices with average $A_{\mathcal{IGP}} = 4/3\sqrt{2\log N/k} > A_{\mathcal{LAS}}$. Additionally, they proved that for averages larger than at least $A_{\text{OGP}} = 5/(3\sqrt{3})\sqrt{\log N/k} > A_{\mathcal{IGP}}$ the problem satisfies the Overlap Gap Property (OGP) [20]. This means that i) the \mathcal{LAS} threshold $A_{\mathcal{LAS}}$ seems to be an algorithm-specific threshold, and not a more general trace of an intrinsic computational-to-statistical gap,

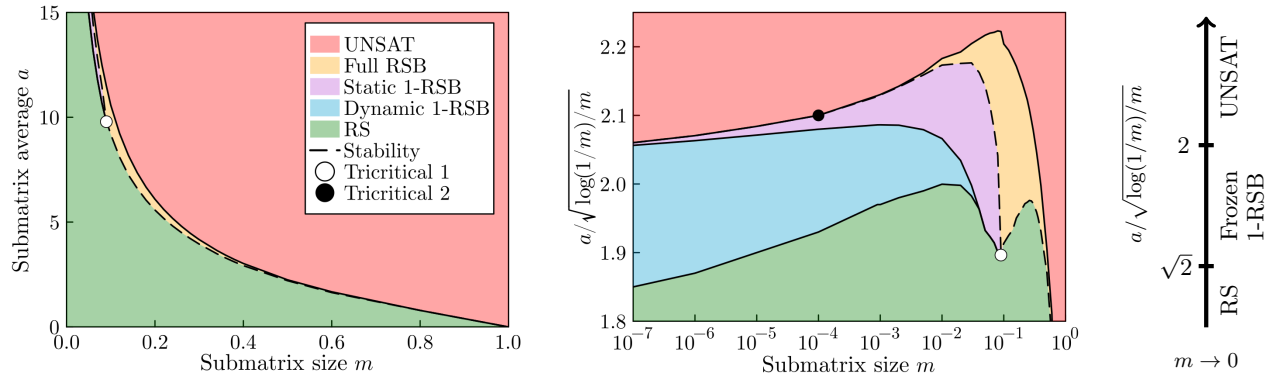


FIG. 1. The phase diagram of the MAS problem as a function of the submatrix-average a and the submatrix size $m = k/N$ for linear scale in m (left), logarithmic scale in m (center) and $m \rightarrow 0$ (right). In the central and right panel we rescale the sub-matrix average as $a/\sqrt{\log(1/m)/(m)}$ to highlight the convergence to the limit. We identify five distinct phases. In the RS phase (green) the system is replica symmetric. In the 1-RSB phases replica symmetry is broken to one step and two sub-phases exists, a dynamical 1-RSB with an extensive number of equilibrium pure states (blue) and a static 1-RSB with only finitely many pure state (purple). In the full-RSB phase (orange) replica symmetry is completely broken and the set of pure states manifests ultrametricity. In the unsatisfiable phase (UNSAT, red) no submatrix exists with the given values of a and m . The transition from RS and 1-RSB to full-RSB is continuous and caused by an instability of the 1-RSB ansatz (dashed line), while the other transitions are discontinuous. We observe two tricritical points, one at (m_c, a_c) where the system shows coexistence of RS, 1-RSB and full-RSB phase (white marker), and one at (m^*, a^*) where the largest-average submatrices become 1-RSB stable and the full-RSB region ceases to exist (black marker). In the limit $m \rightarrow 0$, we observe only the RS, 1-RSB and UNSAT phases. The 1-RSB phase is frozen, meaning that the internal entropy of each pure state goes to zero in the $m \rightarrow 0$ limit.

and ii) that the problem will likely exhibit a hard phase preventing algorithms to find submatrices with averages larger than at least A_{OGP} .

I. THE MODEL

We consider an $N \times N$ random matrix J composed of i.i.d. entries with zero mean and unit variance. A submatrix of J is defined by row and column sets $I, J \subseteq \{1 \dots N\}$ such that the element J_{ij} belongs to the submatrix only if $i \in I$ and $j \in J$. We consider J to be symmetric, and we study principal submatrices, i.e. submatrices whose row-set and column-set coincide $I = J$. The thermodynamics and the thresholds we will obtain are insensitive to this choice, as we argue in the SM. We encode principal submatrices, i.e. their row/column index set I , as Boolean vectors $\sigma = \{\sigma_i\}_{i=1}^N \in \{0, 1\}^N$ such that, if $i \in I$ then $\sigma_i = 1$ and vice versa. We fix the size of the submatrix to $k = mN$, which in the Boolean representation translates to the condition $\sum_i \sigma_i = mN$. We call $m \in (0, 1)$ magnetization. The average of the entries of a submatrix σ can be then expressed as

$$A = |\sigma| = \frac{1}{m^2 N^2} \sum_{i,j=1}^N J_{ij} \sigma_i \sigma_j. \quad (1)$$

We define $a = A\sqrt{N}$, and we will see that a is of order one in the thermodynamic limit.

We probe the energy landscape of the MAS problem

by studying the associated Gibbs measure

$$p(\sigma) = e^{\beta E(\sigma) + \beta h \sum_{i=1}^N \sigma_i} / Z(\beta, h), \quad (2)$$

where β is an inverse temperature that we use to fix the average energy, h is a magnetic field that we use to fix the magnetization m and $Z(\beta, h)$ is the partition function. The energy function is defined as

$$E(\sigma) = \frac{1}{\sqrt{N}} \sum_{i < j} J_{ij} \sigma_i \sigma_j = \frac{m^2 N}{2} a, \quad (3)$$

which, modulo subleading contributions coming from the diagonal term, is a multiple of the submatrix average a .

As the considered model resembles the classic SK model, note that the mapping of the Boolean spins to ± 1 spins, i.e. $s = 2\sigma - 1$, leads to an SK model in a random magnetic field, with couplings correlated to the magnetic field. Such a model has not been considered in the physics literature as far as we are aware.

We will compute all thermodynamic observables through the *quenched free entropy*, i.e. $\Phi = \lim_{N \rightarrow \infty} \mathbb{E}_J \log Z(\beta, h)/N$ where \mathbb{E}_J denotes averaging over the distribution of J . We will see that the free entropy can be expressed as a variational problem for the *overlap* order parameter, which is defined as $q = N^{-1} \sum_{i=1}^N \sigma_i^a \sigma_i^b \in [0, m]$ for two replicas of the system σ^a and σ^b .

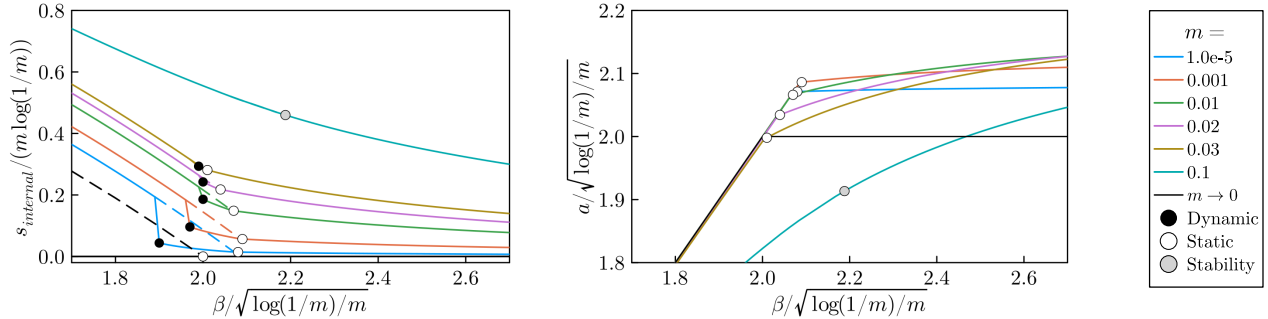


FIG. 2. Behavior of the internal entropy (left panel, solid lines), total entropy (left panel, dashed lines) and the submatrix average (right panel) as a function of the rescaled inverse temperature $\beta/\sqrt{\log(1/m)/m}$ for various values of m . In black, we plot the analytical predictions for the $m \rightarrow 0$ limit. We see that both observables converge to the $m \rightarrow 0$ limit extremely slowly, in accordance with our analytical analysis that shows that the next-to-leading order in the $m \ll 1$ expansion is only logarithmically small, see SM. Moreover, we see that the internal entropy in the dynamical 1-RSB region (where it is different from the total entropy due to the non-vanishing complexity) decreases as m goes to zero, foreshadowing the frozen 1-RSB phase that arises in the limit $m \rightarrow 0$.

II. REPLICA ANALYSIS OF THE FREE ENTROPY

We compute the quenched free entropy Φ using the replica formalism [11], i.e. by using the replica trick $\mathbb{E}_J \log Z = \lim_{n \rightarrow 0} (\mathbb{E}_J Z^n - 1)/n$, computing $\mathbb{E}_J Z^n$ for integer values of n and performing an analytical continuation to take the $n \rightarrow 0$ limit. We perform the analytical continuation under the one-step Replica Symmetry Breaking (1-RSB) ansatz, in which we assume that the Gibbs measure decomposes into a 2-level hierarchy of pure states. After a derivation detailed in the SM, we obtain the following variational free entropy:

$$\begin{aligned} \Phi_{1\text{-RSB}}(m, q_0, q_1, p) &= \\ &= -\frac{\beta^2}{4} [m^2 + (p-1)q_1^2 - pq_0^2] \\ &+ \frac{1}{p} \int Du \log \left[\int Dv \left[1 + e^{\beta H(u,v)} \right]^p \right], \end{aligned} \quad (4)$$

$$H(u, v) = h + \frac{\beta}{2} (m - q_1) + \sqrt{q_0} u + \sqrt{q_1 - q_0} v,$$

where Du and Dv denote integration against a standard Gaussian measure. The variational free entropy depends on the submatrix size/magnetization m , the intra-state overlap q_1 , the inter-state overlap q_0 and the Parisi parameter p . To obtain the equilibrium free entropy we extremize the variational free entropy over m, q_0 and q_1 . The Parisi parameter must be set to one if the resulting complexity (whose definition we provide in the following) is positive, otherwise, the variational free entropy must also be extremized over p . We perform this whole procedure numerically at fixed m as detailed in the Supplementary Material (SM).

In the 1-RSB approximation, we have the following expressions for the observables, to be evaluated at the

equilibrium values of the order parameters. The average energy density (and the submatrix average) equals

$$e = \frac{m^2}{2} a = \frac{\beta}{2} [m^2 + (p-1)q_1^2 - pq_0^2], \quad (5)$$

the total entropy (logarithm of the number of microstates) equals

$$s_{\text{total}} = \Phi - \beta hm - \beta e, \quad (6)$$

and the complexity (logarithm of the number of pure states contributing to the Gibbs measure) equals

$$\Sigma = \max \left(0, \partial_p \left[\underset{m, q_0, q_1}{\text{extr}} \Phi_{1\text{-RSB}} \right]_{p=1} \right). \quad (7)$$

If the complexity is non-zero, the total entropy decomposes as $s_{\text{total}} = s_{\text{internal}} + \Sigma$, where the internal entropy s_{internal} is the logarithm of the number of microstates contributing to each of the exponentially many pure states.

Finally, we need to ensure that the 1-RSB approximation is consistent. This can be checked by a stability analysis of the 1-RSB ansatz against perturbation of higher-order RSB nature. We perform the so-called Type-I stability analysis (see SM Section I.d), obtaining the stability condition

$$\int Du \frac{\int Dv (1 + e^{\beta H})^p [\ell(\beta H)^2 (1 - \ell(\beta H))^2]}{\int Dv (1 + e^{\beta H})^p} < \frac{1}{\beta^2}, \quad (8)$$

where $\ell(x) = 1/(1 + \exp(-x))$.

We derived the replicated free entropy using the replica trick. Note, however, that the proof of the full-RSB free entropy from [19] applies to the MAS problem and thus

our setting. In order to apply their result to our model we note that [19] constrain the free-entropy to fixed self-overlap $q_{\text{self}} = N^{-1} \sum_i \sigma_i^2$, while we constrain the model to fixed magnetization $m = N^{-1} \sum_i \sigma_i$. Due to the choice of Boolean spins, we have that $\sigma_i^2 = \sigma_i$, so that the two constraints coincide (this is not true in general).

III. THE PHASE DIAGRAM

After solving the above equations, we identify five distinct phases for finite $m \in (0, 1)$, and we plot them in Figure 1.

RS phase — For small submatrix-average (corresponding to large temperatures) we observe a replica-symmetric (RS) phase, in which the extremum of the variational free entropy is attained at $q_0^* = q_1^*$. In this phase, the complexity is zero, while the total entropy is strictly positive. As the submatrix average increases (i.e. the temperature is lowered), the system undergoes a phase transition to a replica-symmetry-broken phase. The nature of the transition is different for $m \leq m_c$ and $m \geq m_c$. We start discussing the former case.

Dynamical 1-RSB phase — For $m \leq m_c$, we observe a discontinuous transition at a value $a_{\text{dynamic}}(m)$ of the sub-matrix average from the RS phase to a dynamical 1-RSB phase, in which the extremum of the variational free entropy satisfies $q_0^* \neq q_1^*$. This transition is identified by a sharp jump of the complexity from zero to a positive value, meaning that the measure shatters into an exponential number of pure states each with non-zero entropy. As m decreases, the appropriately rescaled internal entropy decreases, suggesting that in the $m \rightarrow 0$ limit, this phase becomes a frozen 1-RSB phase, see Figure 2 left panel.

Static 1-RSB phase — For $m \leq m_c$, in the dynamical 1-RSB phase, the complexity continuously decreases as the submatrix average $a_{\text{static}}(m) > a_{\text{dynamic}}(m)$ at which the complexity vanishes we observe a first-order phase transition, from the dynamical 1-RSB phase to a static 1-RSB phase ($q_0^* \neq q_1^*$, zero complexity, positive entropy).

Full-RSB phase — For values $m \geq m_c$ we observe a continuous phase transition from RS to full-RSB phase at $a_{\text{stability}}(m)$. The transition happens when the Type-I 1-RSB stability condition (8) fails. We conjecture that this phase is fully replica-symmetry-broken by the similarity to the SK model, in which a similar continuous phase transition to full-RSB occurs. The full-RSB phase is present at all finite values of the magnetization $m \geq m_c$, even though in Figure 1 it is difficult to see it. We provide evidence for this in the SM. For values of $m_c \geq m \geq m^*$, we observe a Gardner-like phase transition at a value $a_{\text{stability}}(m)$ of the sub-matrix average from the 1-RSB phase to a full-RSB phase. This transition is reminiscent of the one known from the Ising p -spin model [21].

UNSAT phase — As the average of the matrix increases, we encounter a point at which the total en-

tropy vanishes, denoting that the sub-matrix average has reached its maximum value $a_{\text{max}}(m)$. After this point, the total entropy becomes negative and we observe an unsatisfiable (UNSAT) phase, where no submatrix with that value of the submatrix-average exists. For $m \geq m^*$, we estimated $a_{\text{max}}(m)$ in the 1-RSB approximation even though this ansatz is unstable in this phase by computing the 1-RSB entropy, finding the temperature at which it vanishes, and computing the corresponding submatrix average. It is often the case that the 1-RSB prediction for the maximum energy is numerically very close to the full-RSB prediction. Evaluation of the full-RSB equations is left for future work.

Tricritical points — The phase diagram features two tricritical points. The first one, at $(m_c, a_c) \approx (0.09 - 0.1, 9.3 - 9.7)$ marks the coexistence of the RS, 1-RSB and full-RSB phases. It can be pinpointed by finding the intersection of the stability and the static transition lines. As $m \rightarrow m_c^-$, the static and dynamic transitions approach very quickly so that it is very difficult to distinguish them numerically. The second tricritical point is at $(m^*, a^*) \approx (0.0001 - 0.002, 100 - 650)$, marking the crossing between the stability and the UNSAT transition lines. For $m \leq m^*$ the 1-RSB phase is stable up to the maximum average $a_{\text{max}}(m)$. This second tricritical point is hard to pinpoint numerically accurately. In the SM, we show analytically that at least for $m \rightarrow 0$ the 1-RSB phase is indeed stable up to $a_{\text{max}}(m)$. Thus, by continuity, this second tricritical point must exist.

IV. THE SMALL MAGNETIZATION LIMIT

We now study the phase diagram in the $m \rightarrow 0$ limit, corresponding to the $k \ll N$ regime. The limit must be taken carefully in order to preserve the extensivity of the energy function in the thermodynamic limit. Indeed, we have that for fixed m and N

$$\text{var}(E(\sigma)) = \mathcal{O}(m^2 N), \quad \# = \mathcal{O}(Nm \log 1/m), \quad (9)$$

where $\#$ denotes the logarithm of the number of microstates at fixed m and N . As $m \rightarrow 0$, the energy must be rescaled by $c(m) = \sqrt{\log(1/m)/m}$, and the entropy and complexity must be rescaled by $m \log(1/m)$. This can be achieved by considering the $m \rightarrow 0$ limit of (4) at fixed $b = \beta/c(m)$. We perform analytically the limit in the RS and 1-RSB approximations, leading to the following phase diagram.

RS phase — For sub-matrix average $a < a_{\text{dynamic}} = \sqrt{2} c(m)$, we observe a stable RS phase with zero complexity and positive total entropy. In this phase, $q_0 = q_1 = m^2$.

Frozen 1-RSB phase — For sub-matrix average $a_{\text{dynamic}} < a < a_{\text{static}} = 2c(m)$, we observe a stable 1-RSB phase with $q_1 = m$, $q_0 = m^2$ and complexity $\Sigma = 1 - b^2/4$. This is a frozen phase, meaning that each of the exponentially-many pure states contributing to the measure has zero internal entropy.

UNSAT phase — For sub-matrix average $a > a_{\text{static}}$, the total entropy is negative, signalling the onset of the UNSAT phase.

The threshold a_{dynamic} and a_{static} coincide with the thresholds proved in [3] for, respectively, the submatrix-average of the local maxima $A_{\text{LAS}} = a_{\text{dynamic}}/\sqrt{N}$ and the maximum submatrix-average achievable $A_{\text{opt}} = a_{\text{static}}/\sqrt{N}$. Thus, as a byproduct of our analysis, we obtain an equilibrium interpretation of A_{LAS} as a freezing transition.

The $m \rightarrow 0$ limit of the MAS phase diagram resembles closely that of the Random Energy Model (REM) [12]. More precisely, we find that the static threshold, as well as the values of the entropy and complexity, do coincide (in the REM the static transition threshold equals $a_{\text{static,REM}} = 2$, the complexity equals $\Sigma = 1 - b^2/4$ and the internal entropy is zero for all $b > 0$). This connection is related to the fact that the MAS energy $E(\sigma)$ is a Gaussian random variable with covariance $\langle E(\sigma)E(\sigma') \rangle \propto q(\sigma, \sigma') \leq m$, which vanishes in the $m \rightarrow 0$ limit. The notable difference between the REM and the MAS problem is given by the finite value of the dynamic threshold in the MAS problem, while in the REM the system is frozen at all temperatures.

In [4], the authors introduced an algorithm called \mathcal{IGP} , and they proved that it can find submatrices with average A which, following our analysis, are inside the frozen 1-RSB region. This is at odds with the common belief that solutions in frozen states are algorithmically hard to find [15]. Another problem in which a similar situation happens is the binary perceptron, where the algorithmic feasibility was explained in relation to out-of-equilibrium dense regions [16, 17]. We leave for future work a deeper understanding of the out-of-equilibrium properties of the MAS problem, and more generally the relation between them and algorithmic tractability.

V. CONCLUSIONS

In this paper, we studied the maximum average submatrix problem using tools from the statistical physics of disordered systems, and in particular a mapping onto a variant of the SK model.

We unveiled the phase diagram in the large submatrix regime $k = mN$, discovering a rich phenomenology including glassy phases, and phases where exponentially-many pure states contribute to the equilibrium behavior of the system.

By considering the $m \rightarrow 0$ limit, we characterized the phase diagram in the small submatrix regime $k \ll N$, shedding some light on previous results [3, 4] and highlighting a connection to the Random Energy model. We note that there exist efficient algorithms that work in the frozen 1-RSB phase, usually associated with hard-algorithmic phases, similar to what happens in the binary perceptron due to non-equilibrium phenomena.

Our findings leave many questions to be answered, such as i) the study of the out-of-equilibrium properties of the problem and their relation with algorithmic hardness and ii) how for $k \ll N$ the vanishingly small correlations between the energies combine to shift the dynamical temperature from infinity (REM) to finite (MAS).

We conclude by remarking that our techniques generalise straightforwardly to the case in which the entries of J are non-Gaussian as long as they are i.i.d. with finite first and second moment, and to the rectangular MAS problem, in which both J and the submatrices may be rectangular possibly with different aspect ratios.

ACKNOWLEDGMENTS

We acknowledge funding from the Swiss National Science Foundation grants 200021-200390 (OperaGOST) and TMPFP2_210012.

[1] A. A. Shabalin, V. J. Weigman, C. M. Perou, and A. B. Nobel, Finding large average submatrices in high dimensional data, *The Annals of Applied Statistics* **3**, 985 (2009).

[2] S. Madeira and A. Oliveira, Bioclustering algorithms for biological data analysis: a survey, *IEEE/ACM Transactions on Computational Biology and Bioinformatics* **1**, 24 (2004).

[3] S. Bhamidi, P. S. Dey, and A. B. Nobel, Energy landscape for large average submatrix detection problems in gaussian random matrices, *Probability Theory and Related Fields* **168**, 919 (2017).

[4] D. Gamarnik and Q. Li, Finding a large submatrix of a Gaussian random matrix, *The Annals of Statistics* **46**, 2511 (2018).

[5] X. Sun and A. B. Nobel, On the maximal size of large-average and anova-fit submatrices in a gaussian random matrix, *Bernoulli: official journal of the Bernoulli Society for Mathematical Statistics and Probability* **19**, 275 (2013).

[6] D. Sherrington and S. Kirkpatrick, Solvable model of a spin-glass, *Physical review letters* **35**, 1792 (1975).

[7] Y. Fu and P. W. Anderson, Application of statistical mechanics to np-complete problems in combinatorial optimisation, *Journal of Physics A: Mathematical and General* **19**, 1605 (1986).

[8] M. Mézard and G. Parisi, Mean-field equations for the matching and the travelling salesman problems, *Europhysics Letters* **2**, 913 (1986).

[9] L. Zdeborová and F. Krzakala, Phase transitions in the coloring of random graphs, *Physical Review E* **76**, 031131 (2007).

[10] M. Mézard, G. Parisi, and R. Zecchina, Analytic and algorithmic solution of random satisfiability problems, *Sci-*

ence **297**, 812 (2002).

[11] M. Mézard, G. Parisi, and M. A. Virasoro, *Spin glass theory and beyond: An Introduction to the Replica Method and Its Applications*, Vol. 9 (World Scientific Publishing Company, 1987).

[12] B. Derrida, Random-energy model: An exactly solvable model of disordered systems, *Physical Review B* **24**, 2613 (1981).

[13] W. Krauth and M. Mézard, Storage capacity of memory networks with binary couplings, *Journal de Physique* **50**, 3057 (1989).

[14] O. Martin, M. Mézard, and O. Rivoire, Frozen glass phase in the multi-index matching problem, *Physical review letters* **93**, 217205 (2004).

[15] D. Gamarnik, C. Moore, and L. Zdeborová, Disordered systems insights on computational hardness, *Journal of Statistical Mechanics: Theory and Experiment* **2022**, 114015 (2022).

[16] C. Baldassi, A. Ingrosso, C. Lucibello, L. Saglietti, and R. Zecchina, Subdominant dense clusters allow for simple learning and high computational performance in neural networks with discrete synapses, *Physical review letters* **115**, 128101 (2015).

[17] C. Baldassi, C. Borgs, J. T. Chayes, A. Ingrosso, C. Lucibello, L. Saglietti, and R. Zecchina, Unreasonable effectiveness of learning neural networks: From accessible states and robust ensembles to basic algorithmic schemes, *Proceedings of the National Academy of Sciences* **113**, E7655 (2016).

[18] P. Chaudhari, A. Choromanska, S. Soatto, Y. LeCun, C. Baldassi, C. Borgs, J. Chayes, L. Sagun, and R. Zecchina, Entropy-sgd: Biasing gradient descent into wide valleys, *Journal of Statistical Mechanics: Theory and Experiment* **2019**, 124018 (2019).

[19] D. Panchenko, Free energy in the mixed p -spin models with vector spins, *The Annals of Probability* **46**, 865 (2018).

[20] D. Gamarnik, The overlap gap property: A topological barrier to optimizing over random structures, *Proceedings of the National Academy of Sciences* **118**, e2108492118 (2021).

[21] E. Gardner, Spin glasses with p -spin interactions, *Nuclear Physics B* **257**, 747 (1985).

[22] H. Nishimori, *Statistical Physics of Spin Glasses and Information Processing: An Introduction* (Oxford University Press, 2001).

Supplemental Materials

I. THE 1-RSB APPROXIMATION

a. Variational free entropy — To derive the variational free entropy (4), one can follow the derivation for the SK model presented in [22]. The only difference in our case is that $\sigma^2 = \sigma$ as $\sigma \in \{0, 1\}$, contrary to the usual case $\sigma_{\text{SK}}^2 = 1$ as $\sigma_{\text{SK}} \in \{-1, +1\}$. The extremization conditions are

$$\begin{aligned} m &= \int Du \frac{\int Dv \text{ logistic}(\beta H)(1 + e^{\beta H})^p}{\int Dv (1 + e^{\beta H})^p}, \\ q_0 &= \int Du \left[\frac{\int Dv \text{ logistic}(\beta H)(1 + e^{\beta H})^p}{\int Dv (1 + e^{\beta H})^p} \right]^2, \\ q_1 &= \int Du \frac{\int Dv \text{ logistic}^2(\beta H)(1 + e^{\beta H})^p}{\int Dv (1 + e^{\beta H})^p}, \\ \Sigma(p) &= p^2 \frac{\beta^2(q_1^2 - q_0^2)}{4} - p \int Du \frac{\int Dv \log 1p\exp(\beta H)(1 + e^{\beta H})^p}{\int Dv (1 + e^{\beta H})^p} + \int Du \log \left[\int Dv (1 + e^{\beta H})^p \right], \end{aligned} \quad (\text{S1})$$

where $\text{logistic}(x) = (1 + e^{-x})^{-1}$ and $H(u, v) = h + \frac{\beta}{2}(m - q_1) + \sqrt{q_0}u + \sqrt{q_1 - q_0}v \equiv H_{1\text{-RSB}}$. We highlighted that the extremization condition inn p is equivalent to imposing zero complexity. Their derivation requires the usage of integration by parts repeatedly, in the form

$$\int Du u f(u) = \int Du f'(u). \quad (\text{S2})$$

b. Observables — To derive the expressions for the energy e (5) and total entropy s (6) in the 1-RSB approximation, use the grand-canonical thermodynamic relations $e = \partial_\beta \Phi - hm$ and $\Phi(\beta) = s + \beta e + \beta hm$. Applying these relations to the variational free entropy (4) produces the equations presented in the text, to be evaluated then at the equilibrium values of the order parameters.

c. Complexity — To derive the expression for the complexity Σ (7) in the 1-RSB approximation, we follow [cite](#). We start by introducing a deformed partition function

$$Z(p) = \sum_\alpha Z_\alpha^p = \sum_\alpha e^{Np\phi_\alpha} = \sum_\phi e^{N(p\phi + \Sigma(\phi))} = e^{N \text{extr}_{\phi: \Sigma(\phi) \geq 0}(p\phi + \Sigma(\phi))}, \quad (\text{S3})$$

where p is just a weighting parameter — at $p = 1$ we are computing the usual partition function Z — and the sum over α runs over all pure states contributing to the Gibbs measure, each with free entropy ϕ_α . One can interpret p as being a number of replicas of our system that are constrained to be in the same pure state, and $Z(p)$ would then be the correct partition function for such replicated system. Thus, we have $\mathbb{E} \log Z(p)/N \sim p\Phi_{1\text{-RSB}}(p)$, where the factor p matches the number of replicas used on the two sides of the equation. Now, the extremization over ϕ on the left-hand side can be performed explicitly, and the extremizer $\phi_*(p)$ satisfies

$$\begin{cases} p + \Sigma'(\phi_*(p)) = 0 & \text{if } \Sigma(\phi_*(p)) \geq 0, \\ \Sigma(\phi_*(p)) = 0 & \text{otherwise.} \end{cases} \quad (\text{S4})$$

Where $\Sigma(\phi_*(p)) \geq 0$

$$\partial_p \Phi_{1\text{-RSB}}(p) = \partial_p \frac{p\phi_*(p) + \Sigma(\phi_*(p))}{p} = \frac{p^2 \partial_p \phi_*(p) + p\Sigma'(\phi_*) \partial_p \phi_*(p) - \Sigma(\phi_*(p))}{p^2} = -\frac{\Sigma(\phi_*(p))}{p^2}, \quad (\text{S5})$$

so that

$$\Sigma(\phi_*(p)) = -p^2 \partial_p \Phi_{1\text{-RSB}}(p). \quad (\text{S6})$$

Plugging $p = 1$, corresponding to the equilibrium partition function, we get

$$\Sigma(\phi_*) = \max(0, -\partial_p \Phi_{1\text{-RSB}}(p = 1)). \quad (\text{S7})$$

d. Stability — The most general stability condition for the k -RSB approximation can be derived by computing the Hessian at the k -RSB equilibrium of the n -replicas free-entropy. A detailed derivation for the RS approximation ($q_0 = q_1$) of the SK model can be found in [22, Chapter 3]. By adapting it to our model, it is easy but tedious to see that the the RS stability condition

$$\beta^2 \int Du \text{ logistic}(\beta H_{\text{RS}})^2 (1 - \text{logistic}(\beta H_{\text{RS}}))^2 < 1, \quad (\text{S8})$$

where $H_{\text{RS}}(u) = \sqrt{q}z + h + \frac{\beta}{2}(m - q)$.

For the 1-RSB stability, we check a simpler condition, called Type-I stability. It is the linear stability of the 2-RSB extremization conditions (seen as fixed point iterations for the overlaps) around the 1-RSB fixed point under the perturbation $q_2^{2-\text{RSB}} = q_1^{1-\text{RSB}} + \epsilon$ and $q_{0,1}^{2-\text{RSB}} = q_{0,1}^{1-\text{RSB}}$. We conjecture that this threshold is not just a bound, but the correct one, in analogy with what happens in the SK model. In practice, we consider the equation for q_2 in the 2-RSB approximation, i.e.

$$q_2 = \int Du \frac{\int Dv \left[\left(\int Dz (1 + e^{\beta H_{2\text{RSB}}})^{p_2} \right)^{p_1/p_2-1} \int Dz (1 + e^{\beta H_{2\text{RSB}}})^{p_2} \text{ logistic}^2(\beta H_{2\text{RSB}}) \right]}{\int Dv \left(\int Dz (1 + e^{\beta H_{2\text{RSB}}})^{p_2} \right)^{p_1/p_2}}, \quad (\text{S9})$$

where $H_{2\text{RSB}}(u, v, z) = h + \frac{\beta}{2}(m - q_2) + \sqrt{q_0}u + \sqrt{q_1 - q_0}v + \sqrt{q_2 - q_1}z$, and we evaluate it at the 1-RSB equilibrium value of the order parameters, i.e. $q_{0,1}^{2-\text{RSB}} = q_{0,1}^{1-\text{RSB}}$ and $p_1^{2-\text{RSB}} = p^{1-\text{RSB}}$ for a perturbation $q_2^{2-\text{RSB}} = q_1^{1-\text{RSB}} + \epsilon$ at fixed 2-step Parisi parameter $p_2^{2-\text{RSB}} \in (p^{1-\text{RSB}}, 1)$. Finally, we expand at first order in ϵ . We report the details of the computation in Section V. The linear stability threshold is the point at which the $\mathcal{O}(\epsilon)$ of the r.h.s. equals 1. This corresponds to the condition (here $p_2^{2-\text{RSB}} = 1$ gives the strictest condition), giving (8).

II. NUMERICAL SOLUTION FOR THE EQUILIBRIUM ORDER PARAMETERS

The numerical solution for the equilibrium order parameters is performed by solving the saddle-point equations

$$\begin{aligned} m &= \int Du \frac{\int Dv \text{ logistic}(\beta H)(1 + e^{\beta H})^p}{\int Dv (1 + e^{\beta H})^p}, \\ q_0 &= \int Du \left[\frac{\int Dv \text{ logistic}(\beta H)(1 + e^{\beta H})^p}{\int Dv (1 + e^{\beta H})^p} \right]^2, \\ q_1 &= \int Du \frac{\int Dv \text{ logistic}^2(\beta H)(1 + e^{\beta H})^p}{\int Dv (1 + e^{\beta H})^p}, \\ \Sigma(p) &= p^2 \frac{\beta^2(q_1^2 - q_0^2)}{4} - p \int Du \frac{\int Dv \text{ log1pexp}(\beta H)(1 + e^{\beta H})^p}{\int Dv (1 + e^{\beta H})^p} + \int Du \log \left[\int Dv (1 + e^{\beta H})^p \right], \end{aligned} \quad (\text{S10})$$

where $\text{logistic}(x) = (1 + e^{-x})^{-1}$ and $H(u, v) = h + \frac{\beta}{2}(m - q_1) + \sqrt{q_0}u + \sqrt{q_1 - q_0}v$. There are several aspects that must be explained.

a. What to do with the Parisi parameter p — The complexity prescribes that at equilibrium $p = 1$ if the associated complexity is positive, and otherwise $p = p^*$ such that $\Sigma(p^*) = 0$. We solve the first three equations of (S10) for m, q_0, q_1 at $p = 1$ first and compute the associated complexity. If it is negative, we discard the solution and solve also for $\Sigma(p) = 0$.

b. How to solve (S10) at fixed p — To solve the first three equations of (S10) for m, q_0, q_1 at fixed p , we could turn them in a fixed-point iteration scheme, as it is done for the SK model. An added element of complexity is that we actually want to fix m , and solve for h . This cannot be done *a posteriori* as the $m(h)$ function at the stable fixed point of the equation is not single-valued (while the inverse $m(h)$ is). Thus, we iterate the equations for q_0 and q_1 as fixed-point equations, and after each iteration we solve the first equation at fixed m for h — by bisection for example — using the current value of the other order parameters. Whenever no solution for h is found, we perturb it with random Gaussian noise of small variance, and reiterate the procedure. Convergence is declared when the relative change in Euclidean norm of the order parameters is below a set tolerance, in our case 10^{-6} .

c. How to solve (S10) imposing $\Sigma(p) = 0$ — We use the same procedure as that described above, but every 3 iterations we also solve $\Sigma(p) = 0$ for p , using the current value of the other order parameters.

d. How to stably compute the integrals in (S10) — To compute the integrals in Du and Dv in the saddle-point equations we use Gauss-Hermite integration, which approximates Gaussian expectations as

$$\int Dz f(z) = \sum_{i=1}^n w_i f(z_i) \quad (\text{S11})$$

for a specific set of weights w_i and base-points z_i . We use $n = 71$, and pre-compute the weights and base-points in advance.

Notice that this integrals can lead to overflows and underflows due to exponential factors. For example, consider the simple RS case $q_0 = q_1$. In this case, all integrals in the v variable drop, as there is no dependence on v anymore, leading to a cancellation of the factors $(1 + \exp(\beta H))^p$. If this cancellation has to happen numerically, it can lead to the aforementioned numerical issues. To solve the equations in a numerically stable way, we work in log-space. We write the integrals as

$$\begin{aligned} & \int Du \frac{\int Dv f(\beta H)(1 + e^{\beta H})^p}{\int Dv (1 + e^{\beta H})^p} \\ &= \int Du \exp \left[\log \int Dv f(\beta H)(1 + e^{\beta H})^p - \log \int Dv (1 + e^{\beta H})^p \right] \\ &= \int Du \exp \left[\log \int Dv \exp [\log f(\beta H) + p \log 1pexp(\beta H)] - \log \int Dv \exp [p \log 1pexp(\beta H)] \right]. \end{aligned} \quad (\text{S12})$$

Now we use that

$$\log \int Dz \exp(f(z)) = \log \sum_{i=1}^n w_i \exp(f(z_i)) = \log \sum_{i=1}^n \exp(f(z_i) + \log w_i) = \text{logsumexp}(\{f(z_i) + \log w_i\}_{i=1}^n). \quad (\text{S13})$$

where stable logsumexp functions are routinely implemented in many programming languages. The idea of the logsumexp trick is to write

$$\log \sum_i \exp(x_i) = x_* + \log \sum_i \exp(x_i - x_*) \quad (\text{S14})$$

where $x_* = \max_i \{x_i\}$, so that all exponentials have negative argument. This allows to compute the integrals quickly and stably.

e. How to enter the large inverse temperature 1-RSB phase and the dynamical 1-RSB phase In both the large inverse temperature 1-RSB phase and the dynamical 1-RSB phase, the solution of the 1-RSB equations depends highly on the initialization. In the first case, poor initialization leads to non-convergence, while in the second case it leads to convergence to the RS fixed point $q_0 = q_1$, in which the complexity erroneously vanishes. To avoid these problems, we manually find good initializations in the full-RSB region or static 1-RSB respectively, at an inverse temperature just above the relevant phase boundary. We then change slightly β (increasing or decreasing it as needed) and feed the previous solution of the equations as initialization at the new inverse temperature. This allows to go at larger values of β in the first case, and inside the dynamical 1-RSB region in the second case.

f. Extrapolation of the observables to compute the stability and the SAT/UNSAT thresholds In order to compute the stability and SAT/UNSAT thresholds we need to extrapolate the values of the energy, entropy and the stability condition to large values of β , larger than reachable with our numerical methods. All these quantities behave as $\text{const} + \mathcal{O}(\beta)$ corrections in the physically relevant region (deep in the unstable phase this is not necessarily true anymore for the stability condition). Thus, we fit the large inverse temperature tails of said observables to the $\text{const} + \mathcal{O}(\beta)$ asymptotics, and estimate the stability and SAT/UNSAT thresholds on this extrapolated data as the points at which, respectively, the stability condition is not satisfied and the entropy becomes negative.

g. Estimation of the dynamic and static transitions We estimate the dynamic and static transition by considering the complexity (at $p = 1$), and computing i) where it first develops a discontinuity jumping from zero to positive as a function of β , and ii) where it firsts continuously evolves from positive to negative. To properly threshold for these events, it is important to rescale the complexity with its natural scaling $m \log(1/m)$ (see the main-text discussion for a justification of this scaling).

h. The full-RSB phase is present at all values of m While in Figure 1 it is difficult to see it, we believe that the full-RSB region survives at all finite values of m . The shrinking of this region is due to the fact that the energy at the stability transition at that at the SAT/UNSAT transition are very close, even though the corresponding values of inverse temperature are not. Figure S1 shows this phenomenon at $m = 0.8$.

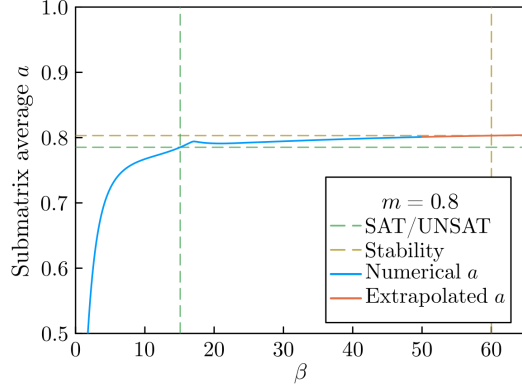


FIG. S1. Submatrix average vs inverse temperature for $m = 0.8$. A large gap between the inverse temperature of the stability and SAT/UNSAT transitions translates to a tiny gap in the submatrix average.

III. THE SMALL MAGNETIZATION LIMIT FOR THE SYMMETRIC MODEL

A. The scaling limit of the RS approximation

We start by considering the RS equations

$$\begin{aligned} m &= \int Du \text{ logistic}(\beta H), \\ q &= \int Du \text{ logistic}(\beta H)^2, \\ H_{\text{RS}} &= h + \sqrt{q}u + \frac{\beta}{2}(m - q), \end{aligned} \tag{S15}$$

in the scaling limit

$$\begin{aligned} \beta &= b\sqrt{\frac{1}{m} \log \frac{1}{m}}, \\ h &= \eta\sqrt{m \log \frac{1}{m}}. \end{aligned} \tag{S16}$$

Then

$$\beta H_{\text{RS}} = b \left(\eta + \frac{b}{2} \left(1 - \frac{q}{m} \right) \right) \log \frac{1}{m} + ub\sqrt{\frac{q}{m} \log \frac{1}{m}}. \tag{S17}$$

We notice here that if $q = cm^{1+\alpha}$, with $c > 0$ and $\alpha > 0$ due to $0 \leq q \leq m$, the second term goes to zero and can be safely neglected. The dependence on u drops, and the saddle point equations imply self-consistently

$$q = \text{logistic}(\beta H_{\text{RS}})^2 = m^2 \implies c = \alpha = 1. \tag{S18}$$

The first equation reads

$$m = \text{logistic} \left(b \left(\eta + \frac{b}{2} \right) \log \frac{1}{m} \right) \implies \log \frac{m}{1-m} = b \left(\eta + \frac{b}{2} \right) \log \frac{1}{m}, \tag{S19}$$

from which

$$\eta = - \left(\frac{1}{b} + \frac{b}{2} \right). \tag{S20}$$

The energy density equals (we consider the symmetric model here, but for the non-symmetric model the computations are analogous)

$$e = \frac{\beta}{2}(m^2 - q^2) \sim \frac{b}{2} \sqrt{\frac{1}{m} \log \frac{1}{m}}. \quad (\text{S21})$$

Given the *a posteriori* knowledge that the small temperature phase is a 1-RSB phase, we can also access the values of the observables in the frozen 1-RSB phase by

- computing $b_{\text{stability}}$ as the value of b at which the entropy density becomes negative;
- computing the observables at $b_{\text{stability}}$, as in the 1-RSB phase they do not depend on the temperature anymore.

Thus, we have (recall $q \ll m$)

$$\begin{aligned} \mathbb{E}\langle e \rangle &\sim -\frac{\beta m^2}{2} \\ \Phi &\sim -\frac{\beta^2 m^2}{4} + \log1pexp(\beta H_{\text{RS}}) = -\frac{\beta^2 m^2}{4} + \mathcal{O}(m) \sim -\frac{\beta^2 m^2}{4} \end{aligned} \quad (\text{S22})$$

and the entropy density

$$\mathbb{E}s = \Phi + \beta \mathbb{E}\langle e \rangle - \beta hm = \left(1 + \frac{b^2}{2} - \frac{3b^2}{4}\right) m \log \frac{1}{m} = \left(1 - \frac{b^2}{4}\right) m \log \frac{1}{m} \quad (\text{S23})$$

from which

$$b_{\text{stability}} = 2. \quad (\text{S24})$$

Notice that, modulo a factor \log_2 due a different normalisation of the entropy, the RS $m \rightarrow 0$ limit reproduces exactly the results for the RS solution of the Random Energy Model [12].

B. The scaling limit in the 1RSB approximation: solving the SP equations

We start by considering the 1-RSB equations

$$\begin{aligned} m &= \int Du \frac{\int Dv \text{ logistic}(\beta H)(1 + e^{\beta H})^p}{\int Dv (1 + e^{\beta H})^p} \\ q_0 &= \int Du \left[\frac{\int Dv \text{ logistic}(\beta H)(1 + e^{\beta H})^p}{\int Dv (1 + e^{\beta H})^p} \right]^2 \\ q_1 &= \int Du \frac{\int Dv \text{ logistic}^2(\beta H)(1 + e^{\beta H})^p}{\int Dv (1 + e^{\beta H})^p} \\ \Sigma(p) &= p^2 \frac{\beta^2(q_1^2 - q_0^2)}{4} - p \int Du \frac{\int Dv \log1pexp(\beta H)(1 + e^{\beta H})^p}{\int Dv (1 + e^{\beta H})^p} + \int Du \log \left[\int Dv (1 + e^{\beta H})^p \right] \end{aligned} \quad (\text{S25})$$

where

$$H(u, v) = \sqrt{q_0}u + \sqrt{q_1 - q_0}v + \frac{\beta}{2}(m - q_1) + h \equiv H_{\text{1RSB}}, \quad (\text{S26})$$

and $\Sigma(p)$ is the complexity. The 1-RSB free entropy potential is given by

$$\Phi_{\text{1RSB}} = -\frac{\beta^2}{4} [m^2 + (s-1)q_1^2 - sq_0^2] + \frac{1}{p} \int Du \log \int Dv (1 + e^{\beta H(u, v)})^p. \quad (\text{S27})$$

We consider the scaling limit

$$\begin{aligned} \beta &= b \sqrt{\frac{1}{m} g(m)}, \\ h &= -\mu \sqrt{m g(m)}, \\ q_1 &= c^2 m \quad \text{with} \quad c \in (0, 1], \\ q_0 &= m^2, \\ s &= \mathcal{O}_m(1), \quad s \in (0, 1], \end{aligned} \quad (\text{S28})$$

where

$$g(m) \sim \log \frac{1}{m}, \quad (\text{S29})$$

at leading order. We also assume that $\mu > 0$, in accordance to the RS solution.

We have that

$$\beta H = -b\mu g + \frac{b^2}{2}(1 - c^2)g + bc\sqrt{g}v + b\sqrt{mgu} \quad (\text{S30})$$

and we see that the only term that is going to zero is the last term. Thus, the dependence on u can be dropped, confirming immediately through the second SP equation that $q_0 = m^2$.

The solution of the equation is detailed in the next section III C. Here we summarise the results.

If $c^2g \rightarrow 0$ — happening whenever c goes to 0 polynomially — then the dependence on v drops, and we get $q_1 = m^2$ similarly as it happened for q_0 . This retrieves the RS solution computed in the previous Section.

If $c = \mathcal{O}_m(1)$, then we have $g = -\log m$ to all non-vanishing orders in m , and

$$\mu = \frac{p^2b^2 + 2}{2pb} \quad \text{and} \quad \Sigma(p, b) = \left(1 - \frac{1}{4}p^2b^2\right)m \log \frac{1}{m}, \quad (\text{S31})$$

under the conditions

$$b > \sqrt{2} \text{ and } \sqrt{2} < bp < b + \sqrt{b^2 - 2}. \quad (\text{S32})$$

The equilibrium solution is given by the condition $p = 1$ whenever $\Sigma(b, p = 1) > 0$, and by $\Sigma(b, p) = 0$ otherwise. This gives $p = 1$ for $\sqrt{2} < b < 2$, and $p = 2/b$ for $b > 2$.

- In the region of positive complexity $p = 1$, we have that exponentially many thermodynamic states with the same free entropy contribute to the thermodynamics of the system. We have that

$$\begin{aligned} \Phi &= -\frac{b^2}{4}p m \log \frac{1}{m}, \\ \beta e &= \frac{b^2}{2}p m \log \frac{1}{m}, \\ \beta hm &= -\mu b m \log \frac{1}{m}, \end{aligned} \quad (\text{S33})$$

so that

$$s_{\text{internal}} = \Phi - \beta hm - \Sigma + \beta e = 0 \quad (\text{S34})$$

confirming that this phase is a frozen 1-RSB phase, and

$$a = \frac{2}{m^2 N^{1/2}} e = \frac{2}{m^2 N^{1/2}} \frac{b}{2} m^{3/2} \sqrt{\log \frac{1}{m}} = b \sqrt{\frac{1}{mN} \log \frac{1}{m}}. \quad (\text{S35})$$

In particular, this gives a_{dynamic} and a_{static} by substituting the limits $b = \sqrt{2}$ and $b = 2$.

- In the region of zero complexity $p = 2/b$, and

$$\begin{aligned} \Phi &= -\frac{b}{2} m \log \frac{1}{m}, \\ \beta e &= b m \log \frac{1}{m}, \\ \beta hm &= -\mu b m \log \frac{1}{m}, \end{aligned} \quad (\text{S36})$$

so that

$$a = \frac{2}{m^2 N^{1/2}} e = \frac{2}{m^2 N^{1/2}} m^{3/2} \sqrt{\log \frac{1}{m}} = 2 \sqrt{\frac{1}{mN} \log \frac{1}{m}}, \quad (\text{S37})$$

confirming that for $b > 2$ we have that $a = a_{\text{max}} = a_{\text{stability}}$.

We also find two other solutions. One describes the boundary between the RS and 1-RSB phase, and exists only on a 1d curve in the phase space. The other is a solution with $0 < s < 1$ that is not stable under 2-RSB perturbations, and that could not be reproduced by us by solving numerically the 1-RSB saddle-point equations. We leave a more detailed study for future work.

C. Solution of the 1-RSB SP equations in the scaling limit

We start by noticing that for $c^2 \rightarrow 0$ such that $c^2 g \rightarrow 0$ the dependence on v drops, and we get $q_1 = m^2$ similarly as it happened for q_0 . This retrieves the RS solution. If instead the v dependence does not drop, then we can expect $q_1 = cm$ with $c \neq 0$. Thus, our task is now to solve the remaining three SP equations for μ, c, s at fixed b and for $c \neq 0, \mu > 0$. We will define the auxiliary variables x and y as

$$\begin{aligned} xy &= b\mu - \frac{b^2}{2}(1 - c^2), \\ y &= bc \end{aligned} \quad (\text{S38})$$

for convenience, with $y \neq 0$ and $x > 0$, so that

$$\beta H = -xyg + y\sqrt{g}v. \quad (\text{S39})$$

We need to study integrals of the form

$$\int Dv (1 + e^{\beta H})^p f(\beta H) \quad (\text{S40})$$

where $f(z) = z, \text{logistic}(z), \text{logistic}(z)^2$. Notice that βH is a monotone increasing function of v with unique zero at $v_* = x\sqrt{g} > 0$.

Let's look at the integrals ($\ell = 0, 1, 2$)

$$\int Dv (1 + e^{\beta H})^p \text{logistic}(\beta H)^\ell = \int Dv (1 + e^{\beta H})^{p-\ell} e^{\ell \beta H}. \quad (\text{S41})$$

We have the uniformly convergent expansions

$$\begin{aligned} (1 + e^{\beta H})^{p-\ell} e^{\ell \beta H} &= \sum_{n \geq 0} \binom{p-\ell}{n} e^{-(n+\ell)y x g + (n+\ell)y \sqrt{g} v} \quad \text{for } v < v_*, \\ (1 + e^{\beta H})^{p-\ell} e^{\ell \beta H} &= e^{p \beta H} (1 + e^{-\beta H})^{s-\ell} = \sum_{n \geq 0} \binom{p-\ell}{n} e^{-(p-n)y x g + (p-n)y \sqrt{g} v} \quad \text{for } v > v_*, \end{aligned} \quad (\text{S42})$$

that can be integrated in the respective domains term-by-term giving

$$\begin{aligned} \int_{-\infty}^{v_*} Dv (1 + e^{\beta H})^p \text{logistic}(\beta H)^\ell &= \sum_{n \geq 0} \binom{p-\ell}{n} e^{-(n+\ell)y x g} \int_{-\infty}^{v_*} Dv e^{(n+\ell)y \sqrt{g} v} \\ &= \sum_{n \geq 0} \binom{p-\ell}{n} e^{-(n+\ell)y x g + \frac{1}{2} y^2 (n+\ell)^2 g} G(\sqrt{g}(x - (n+\ell)y)), \\ \int_{v_*}^{+\infty} Dv (1 + e^{\beta H})^p \text{logistic}(\beta H)^\ell &= \sum_{n \geq 0} \binom{p-\ell}{n} e^{-(p-n)y x g} \int_{v_*}^{+\infty} Dv e^{(p-n)y \sqrt{g} v} \\ &= \sum_{n \geq 0} \binom{p-\ell}{n} e^{-(p-n)y x g + \frac{1}{2} y^2 (p-n)^2 g} G(\sqrt{g}((p-n)y - x)), \end{aligned} \quad (\text{S43})$$

where for $g \rightarrow \infty$ we have

$$G(z\sqrt{g}) = \frac{1}{2} \left(1 + \text{erf} \left(\frac{z\sqrt{g}}{\sqrt{2}} \right) \right) \sim \begin{cases} \frac{\kappa(z)}{(\sqrt{2\pi g}|z|)^{-1} \exp(-\frac{z^2}{2}g)} & z \geq 0 \\ 0 & z < 0 \end{cases}, \quad (\text{S44})$$

and $\kappa(z) = 1$ for positive z , $\kappa(0) = 1/2$. Thus

$$\begin{aligned}
\int Dv (1 + e^{\beta H})^p \text{logistic}(\beta H)^\ell &= \sum_{n \geq 0} \binom{p - \ell}{n} e^{-(n+\ell)y x g + \frac{1}{2} y^2 (n+\ell)^2 g} G(\sqrt{g}(x - (n+\ell)y)) \\
&\quad + \sum_{n \geq 0} \binom{p - \ell}{n} e^{-(p-n)y x g + \frac{1}{2} y^2 (p-n)^2 g} G(\sqrt{g}((p-n)y - x)) \\
&= \sum_{n \geq 0} \binom{p - \ell}{n} \begin{cases} \frac{1}{\sqrt{2\pi g}(ny-x+\ell y)} e^{-gx^2/2} & n+\ell > x/y \\ \kappa(x/y - n - \ell) e^{-(n+\ell)y x g + \frac{1}{2} y^2 (n+\ell)^2 g} & n+\ell \leq x/y \end{cases} \\
&\quad + \sum_{n \geq 0} \binom{p - \ell}{n} \begin{cases} \frac{1}{\sqrt{2\pi g}(ny+x-p y)} e^{-gx^2/2} & p-n < x/y \\ \kappa(p-n-x/y) e^{-(p-n)y x g + \frac{1}{2} y^2 (s-n)^2 g} & p-n \geq x/y \end{cases} \\
&= \sum_{n \geq 0} \binom{p - \ell}{n} \begin{cases} \frac{1}{\sqrt{2\pi g}(ny-x+\ell y)} e^{-gf(x/y)} & n+\ell > x/y \\ \kappa(x/y - n - \ell) e^{-gf(n+\ell)} & n+\ell \leq x/y \end{cases} \\
&\quad + \sum_{n \geq 0} \binom{p - \ell}{n} \begin{cases} \frac{1}{\sqrt{2\pi g}(ny+x-s y)} e^{-gf(x/y)} & p-n < x/y \\ \kappa(p-n-x/y) e^{-gf(p-n)} & p-n \geq x/y \end{cases}
\end{aligned} \tag{S45}$$

where $f(z) = zyx - \frac{1}{2}y^2 z^2$, and $f(0) = 0$, $f(x/y) = \max_z f(z) > 0$ and $f(2x/y) = 0$. Knowing that $g = -\log m$ at leading order, we have that the leading terms will be those with smallest coefficient of $-g$. Notice also that the third exponent comes always with an additional factor $1/\sqrt{g}$. Thus, we have that

$$\begin{aligned}
\int Dv (1 + e^{\beta H})^p \text{logistic}(\beta H)^\ell &= \\
&= \sum_{n \geq 0} \binom{p - \ell}{n} \begin{cases} \frac{e^{-gx^2/2}}{\sqrt{2\pi g}} \left[\frac{1}{ny-x+\ell y} + \frac{1}{ny+x-p y} \right] & n+\ell > x/y \text{ and } p-n < x/y \\ \kappa(p-n-x/y) e^{-gf(p-n)} & n+\ell > x/y \text{ and } p-n \geq x/y \\ \kappa(x/y - n - \ell) e^{-gf(n+\ell)} & n+\ell \leq x/y \text{ and } p-n < x/y \\ \kappa(x/y - n - \ell) e^{-gf(n+\ell)} + \kappa(p-n-x/y) e^{-gf(p-n)} & n+\ell \leq x/y \text{ and } p-n \geq x/y \end{cases} \\
&= \sum_{n \geq 0} \binom{p - \ell}{n} \begin{cases} \frac{e^{-gx^2/2}}{\sqrt{2\pi g}} \left[\frac{1}{ny-x+\ell y} + \frac{1}{ny+x-p y} \right] & n > \max(x/y - \ell, p - x/y) \\ \kappa(p-n-x/y) e^{-gf(p-n)} & x/y - \ell < n \leq p - x/y \text{ if } 2x/y < p + \ell \\ \kappa(x/y - n - \ell) e^{-gf(n+\ell)} & s - x/y < n \leq x/y - \ell \text{ if } p + \ell < 2x/y \\ \kappa(x/y - n - \ell) e^{-gf(n+\ell)} + \kappa(p-n-x/y) e^{-gf(p-n)} & n \leq \min(x/y - \ell, p - x/y) \end{cases}
\end{aligned} \tag{S46}$$

Let us now look at the values of ℓ of interest. We have $\ell = 0$

$$\begin{aligned}
\int Dv (1 + e^{\beta H})^p &= \\
&= \sum_{n \geq 0} \binom{p}{n} \begin{cases} \frac{e^{-gx^2/2}}{\sqrt{2\pi g}} \left[\frac{1}{ny-x} + \frac{1}{ny+x-p y} \right] & n > \max(x/y, p - x/y) \\ \kappa(p-n-x/y) e^{-gf(p-n)} & x/y < n \leq p - x/y \text{ if } 2x/y < p \\ \kappa(x/y - n) e^{-gf(n)} & p - x/y < n \leq x/y \text{ if } p < 2x/y \\ \kappa(x/y - n) e^{-gf(n)} + \kappa(p-n-x/y) e^{-gf(p-n)} & n \leq \min(x/y, p - x/y) \end{cases}
\end{aligned} \tag{S47}$$

We consider the following cases:

- if $0 < p < x/y$, only the first and third cases contribute, and the leading term is the $n = 0$ term of the third branch which equals $\kappa(x/y)$. The first correction is the $n = 1$ term of the same branch if $x/y \geq 1$, which is of order $e^{-gf(1)}$, or the $n = 1$ term of the first branch if $0 < x/y < 1$, which is of order $e^{-gx^2/2}/\sqrt{g}$.
- If $x/y \leq p < 2x/y$, the first, third and fourth cases contribute. The $e^{-gf(n)}$ term has contributions from the third and fourth branches, and $n \leq x/y$ implies that the dominant term is $n = 0$, which equals $\kappa(x/y)$. There is also a contribution from the term $e^{-gf(p-n)}$ for $0 \leq n \leq p - x/y$, whose dominant term is again the $n = 0$ term which is of order $e^{-gf(p)}$. But $x/y \leq p < 2x/y$ implies $f(p) > 0$, so that this term is subleading. Thus, the leading term equals $\kappa(x/y)$, and the first correction is $e^{-g \min(f(p), f(1))}$ if $x/y \geq 1$, or $e^{-gf(p)}$ if $0 < x/y < 1$.

- If $p = 2x/y$ only the first and fourth case contribute. The leading term is the $n = 0$ term of the fourth branch, with both terms contributing equally due to the symmetry $f(z) = f(2x/y - z)$. The leading term is then $2\kappa(x/y)$, and the first correction is either of order $e^{-gf(1)}$ if $x/y \geq 1$, or of order $e^{-gx^2/2}/\sqrt{g}$ if $0 < x/y < 1$.
- If $p > 2x/y$, the first, second and fourth cases contribute. The $e^{-gf(p-n)}$ term has contributions from the second and fourth branches, and the dominant term is given by $n = 0$ as $0 \leq n \leq p - x/y$. Notice that $f(p) < 0$ and that $f(n) > 0$ for $0 \leq n \leq x/y$, so that the $e^{-gf(n)}$ term of the fourth branch is always subleading. Thus, the leading term in this case is given by $\kappa(p - x/y)e^{-gf(p)}$, and the first correction is of order $e^{-g \min(f(p-1), f(0))}$ if $p - x/y \geq 1$, and $e^{-gf(0)}$ if $0 < p - x/y < 1$.

For $\ell = 1$ we have

$$\begin{aligned} & \int Dv (1 + e^{\beta H})^p \text{logistic}(\beta H) \\ &= \sum_{n \geq 0} \binom{p-1}{n} \begin{cases} \frac{e^{-gx^2/2}}{\sqrt{2\pi g}} \left[\frac{1}{ny-x+y} + \frac{1}{ny+x-py} \right] & n > \max(x/y - 1, p - x/y) \\ \kappa(p - n - x/y)e^{-gf(p-n)} & x/y - 1 < n \leq p - x/y \text{ if } 2x/y - 1 < p \\ \kappa(x/y - n - 1)e^{-gf(n+1)} & p - x/y < n \leq x/y - 1 \text{ if } p < 2x/y - 1 \\ \kappa(x/y - n - 1)e^{-gf(n+1)} + \kappa(p - n - x/y)e^{-gf(p-n)} & n \leq \min(x/y - 1, p - x/y) \end{cases} \end{aligned} \quad (\text{S48})$$

We consider the following cases:

- if $0 < x/y < 1$ and $0 < p < x/y$, then only the first branch contributes, and all terms in the sum contribute to leading order. By resummation we have that the leading term equals $K_1 e^{-gx^2/2}/\sqrt{g}$ where

$$K_1 = \frac{1}{\sqrt{2\pi}} \left[\frac{2F_1 \left(1 - p, \frac{x}{y} - p; -p + \frac{x}{y} + 1; -1 \right)}{x - py} - \frac{2F_1 \left(1 - p, 1 - \frac{x}{y}; 2 - \frac{x}{y}; -1 \right)}{x - y} \right]. \quad (\text{S49})$$

- If $0 < x/y < 1$ and $p \geq x/y$, then only the first and second terms contribute. The leading term is given by the $n = 0$ term of the second branch, which equals $\kappa(s - x/y)e^{-gf(p)}$.
- If $x/y \geq 1$ and $0 < p < x/y$, then only the first and third terms contribute. The leading term is given by the $n = 0$ term of the third branch, which equals $\kappa(x/y - 1)e^{-gf(1)}$.
- If $x/y \geq 1$ and $x/y \leq p < 2x/y - 1$, then the first, third and fourth terms contribute. The leading term has order either $e^{-gf(1)}$ or $e^{-gf(p)}$, coming from the $n = 0$ term of the fourth branch. But under these conditions $f(1) < f(p)$ so the leading term is $\kappa(x/y - 1)e^{-gf(1)}$.
- If $x/y \geq 1$ and $p = 2x/y - 1$ then the first and fourth terms contribute. The leading term is the $n = 0$ term of the fourth branch. Under these conditions $f(1) = f(p)$ so the leading term is $2\kappa(x/y - 1)e^{-gf(1)}$.
- If $x/y \geq 1$ and $p > 2x/y - 1$ then the first, second and fourth terms contribute. The leading term has order either $e^{-gf(1)}$ or $e^{-gf(p)}$, coming from the $n = 0$ term of the fourth branch. But under these conditions $f(1) > f(p)$ so the leading term is $\kappa(p - x/y)e^{-gf(p)}$.

For $\ell = 2$ we have

$$\begin{aligned} & \int Dv (1 + e^{\beta H})^p \text{logistic}(\beta H)^2 \\ &= \sum_{n \geq 0} \binom{p-2}{n} \begin{cases} \frac{e^{-gx^2/2}}{\sqrt{2\pi g}} \left[\frac{1}{ny-x+2y} + \frac{1}{ny+x-py} \right] & n > \max(x/y - 2, p - x/y) \\ \kappa(p - n - x/y)e^{-gf(p-n)} & x/y - 2 < n \leq p - x/y \text{ if } 2x/y - 2 < p \\ \kappa(x/y - n - 2)e^{-gf(n+2)} & p - x/y < n \leq x/y - 2 \text{ if } p < 2x/y - 2 \\ \kappa(x/y - n - 2)e^{-gf(n+2)} + \kappa(p - n - x/y)e^{-gf(p-n)} & n \leq \min(x/y - 2, p - x/y) \end{cases} \end{aligned} \quad (\text{S50})$$

We consider the following cases:

- if $0 < x/y < 2$ and $0 < p < x/y$, then only the first term contributes, and all terms in the sum contribute to leading order. By resummation we have that the leading term equals $K_2 e^{-gx^2/2}/\sqrt{g}$ where

$$K_2 = \frac{1}{\sqrt{2\pi}} \left[\frac{{}_2F_1\left(2-p, \frac{x}{y}-p; -p+\frac{x}{y}+1; -1\right)}{x-py} - \frac{{}_2F_1\left(2-p, 2-\frac{x}{y}; 3-\frac{x}{y}; -1\right)}{x-2y} \right]. \quad (\text{S51})$$

- If $0 < x/y < 2$ and $p \geq x/y$, then only the first and second terms contribute. The leading term is given by the $n = 0$ term of the second branch, which equals $\kappa(p - x/y)e^{-gf(p)}$.
- If $x/y \geq 2$ and $0 < p < x/y$, then only the first and third terms contribute. The leading term is given by the $n = 0$ term of the third branch, which equals $\kappa(x/y - 2)e^{-gf(2)}$.
- If $x/y \geq 2$ and $x/y \leq p < 2x/y - 2$, then the first, third and fourth terms contribute. The leading term has order either $e^{-gf(2)}$ or $e^{-gf(p)}$, coming from the $n = 0$ term of the fourth branch. But under these conditions $f(2) < f(p)$ so the leading term is $\kappa(x/y - 2)e^{-gf(2)}$.
- If $x/y \geq 2$ and $p = 2x/y - 2$ then the first and fourth terms contribute. The leading term is the $n = 0$ term of the fourth branch. Under these conditions $f(2) = f(p)$ so the leading term is $2\kappa(x/y - 2)e^{-gf(2)}$.
- If $x/y \geq 2$ and $p > 2x/y - 2$ then the first, second and fourth terms contribute. The leading term has order either $e^{-gf(2)}$ or $e^{-gf(p)}$, coming from the $n = 0$ term of the fourth branch. But under these conditions $f(2) > f(p)$ so the leading term is $\kappa(p - x/y)e^{-gf(p)}$.

Thus (notice that $x/y > 0 \implies \kappa(x/y) = \kappa(x/y + 1) = \kappa(x/y + 2) = 1$)

$$\int Dv (1 + e^{\beta H})^p \sim \begin{cases} 1 & 0 < p < 2x/y \\ 2 & p = 2x/y \\ e^{-gf(p)} & p > 2x/y \end{cases}. \quad (\text{S52})$$

and

$$\int (1 + e^{\beta H})^p \text{logistic}(\beta H) \sim \begin{cases} K_1 e^{-gx^2/2}/\sqrt{g} & 0 < p < x/y \text{ and } 0 < x/y < 1 \\ \kappa(p - x/y)e^{-gf(p)} & p \geq x/y \text{ and } 0 < x/y < 1 \\ \kappa(x/y - 1)e^{-gf(1)} & 0 < p < 2x/y - 1 \text{ and } x/y \geq 1 \\ 2\kappa(x/y - 1)e^{-gf(1)} & p = 2x/y - 1 \text{ and } x/y \geq 1 \\ \kappa(p - x/y)e^{-gf(p)} & p > 2x/y - 1 \text{ and } x/y \geq 1 \end{cases}, \quad (\text{S53})$$

and

$$\int (1 + e^{\beta H})^p \text{logistic}(\beta H)^2 \sim \begin{cases} K_2 e^{-gx^2/2}/\sqrt{g} & 0 < p < x/y \text{ and } 0 < x/y < 2 \\ \kappa(p - x/y)e^{-gf(p)} & p \geq x/y \text{ and } 0 < x/y < 2 \\ \kappa(x/y - 2)e^{-gf(2)} & 0 < p < 2x/y - 2 \text{ and } x/y \geq 2 \\ 2\kappa(x/y - 2)e^{-gf(2)} & p = 2x/y - 2 \text{ and } x/y \geq 2 \\ \kappa(p - x/y)e^{-gf(p)} & p > 2x/y - 2 \text{ and } x/y \geq 2 \end{cases}, \quad (\text{S54})$$

We summarise the leading order asymptotics of the $\ell = 0, 1, 2$ integrals in Table I. We can now solve the SP equations: we list all cases in Table II. We obtain the following solutions:

- case $0 < p < x/y < 1$ (Table II solution (1)): $g = -\log\left(\gamma m \sqrt{\log \frac{1}{m}}\right)$, $x = \sqrt{2}$, $\gamma K_1 = 1$, $\gamma K_2 = c^2$. This solution must be studied numerically.
- Case $2x/y - 1 < p < 2x/y$ and $x/y \geq 1$, or $x/y \leq p < 2x/y$ and $0 < x/y < 1$ (Table II solutions (2, 4, 6)): $g = -\log m/\kappa(s - x/y)$, $c = 1$ (notice that $c = 1 \implies y = b$ and $x = \mu$), $\mu = \frac{p^2 b^2 + 2}{2pb}$, and the conditions reduce to

$$\left(0 < b < \sqrt{2} \text{ and } p > \frac{2}{b^2}\right) \text{ or } \left(b > \sqrt{2} \text{ and } p \geq \frac{\sqrt{2}}{b}\right). \quad (\text{S55})$$

| For $0 < x/y < 1$: | $\ell = 0$ | $\ell = 1$ | $\ell = 2$ |
|---------------------|--------------|-----------------------------|-----------------------------|
| $0 < p < x/y$ | 1 | $K_1 e^{-gx^2/2}/\sqrt{g}$ | $K_2 e^{-gx^2/2}/\sqrt{g}$ |
| $x/y \leq p < 2x/y$ | 1 | $\kappa(p - x/y)e^{-gf(p)}$ | $\kappa(p - x/y)e^{-gf(p)}$ |
| $p = 2x/y$ | 2 | $e^{-gf(p)}$ | $e^{-gf(p)}$ |
| $p > 2x/y$ | $e^{-gf(p)}$ | $e^{-gf(p)}$ | $e^{-gf(p)}$ |

| For $1 \leq x/y < 2$: | $\ell = 0$ | $\ell = 1$ | $\ell = 2$ |
|-------------------------|--------------|------------------------------|-----------------------------|
| $0 < p < x/y$ | 1 | $\kappa(x/y - 1)e^{-gf(1)}$ | $K_2 e^{-gx^2/2}/\sqrt{g}$ |
| $x/y \leq p < 2x/y - 1$ | 1 | $\kappa(x/y - 1)e^{-gf(1)}$ | $\kappa(p - x/y)e^{-gf(p)}$ |
| $p = 2x/y - 1$ | 1 | $2\kappa(x/y - 1)e^{-gf(1)}$ | $\kappa(p - x/y)e^{-gf(p)}$ |
| $2x/y - 1 < p < 2x/y$ | 1 | $e^{-gf(p)}$ | $e^{-gf(p)}$ |
| $p = 2x/y$ | 2 | $e^{-gf(p)}$ | $e^{-gf(p)}$ |
| $p > 2x/y$ | $e^{-gf(p)}$ | $e^{-gf(p)}$ | $e^{-gf(p)}$ |

| For $x/y \geq 2$: | $\ell = 0$ | $\ell = 1$ | $\ell = 2$ |
|---------------------------|--------------|---------------|------------------------------|
| $0 < p < 2x/y - 2$ | 1 | $e^{-gf(1)}$ | $\kappa(x/y - 2)e^{-gf(2)}$ |
| $p = 2x/y - 2$ | 1 | $e^{-gf(1)}$ | $2\kappa(x/y - 2)e^{-gf(2)}$ |
| $2x/y - 2 < p < 2x/y - 1$ | 1 | $e^{-gf(1)}$ | $\kappa(p - x/y)e^{-gf(p)}$ |
| $p = 2x/y - 1$ | 1 | $2e^{-gf(1)}$ | $e^{-gf(p)}$ |
| $2x/y - 1 < p < 2x/y$ | 1 | $e^{-gf(p)}$ | $e^{-gf(p)}$ |
| $p = 2x/y$ | 2 | $e^{-gf(p)}$ | $e^{-gf(p)}$ |
| $p > 2x/y$ | $e^{-gf(p)}$ | $e^{-gf(p)}$ | $e^{-gf(p)}$ |

TABLE I. Summary of the asymptotics of the $\ell = 0, 1, 2$ integrals.

- Case $p = 2x/y - 1$ and $x/y \geq 1$ (Table II solutions (3, 5): $g = -\log m/2\kappa(x/y - 1)$, $c = 1/\sqrt{2}$ (notice that $c = 1/\sqrt{2} \implies b = \sqrt{2}y$ and $\mu = \frac{b+2\sqrt{2}x}{4}$), $\mu = \frac{b^2+2}{2b}$, $p = 4/b^2$, and the conditions reduce to $0 < b \leq 2$.

Figure S2 sums up the solutions, highlighting that the $c^2 = 1/2$ case is just a boundary between the RS and 1-RSB phase.

D. The complexity in the scaling limit

We are now ready to compute the complexity $\Sigma(p, b)$ for all solutions found in the previous section, i.e. under the conditions $0 < s < x/y < 1$ and $2x/y - 1 < s < 2x/y$.

Recall that

$$\Sigma(p, b) = \frac{1}{4}p^2b^2c^4m \log \frac{1}{m} - p \int Dv (1 + e^{\beta H})^p \log \text{1pexp}(\beta H) + \log \int Dv (1 + e^{\beta H})^p \quad (\text{S56})$$

and H in this limit is given by Eq.(S39); so we need to compute the leading asymptotic scaling of

$$\int Dv (1 + e^{\beta H})^p \log \text{1pexp}(\beta H), \quad (\text{S57})$$

and the next-to-leading order of

$$\int Dv (1 + e^{\beta H})^p. \quad (\text{S58})$$

We already argued that the $\ell = 0$ integral equals $1 + o_m(1)$ in all solution branches. More in detail, we have

- for $0 < p < x/y < 1$, the $\ell = 0$ integral equals $1 + m^{-x^2/2} = 1 + m$.

| For $0 < x/y < 1$: | Solution |
|---------------------------|---|
| (1) $0 < p < x/y$ | $g = -\log \left(\gamma m \sqrt{\log \frac{1}{m}} \right), x = \sqrt{2}, \gamma K_1 = 1, \gamma K_2 = c^2$ |
| (2) $x/y \leq p < 2x/y$ | $g = -\log m/\kappa(p - x/y), c = 1, x = \frac{p^2 y^2 + 2}{2py}$ |
| $p = 2x/y$ | $g = -\log 2m, c = 1, x = \frac{p^2 y^2 + 2}{2py} = \frac{4x^2 + 2}{4x} \Rightarrow \text{no solution}$ |
| $p > 2x/y$ | $g = -\log m, f(p) = f(p) + 1 \Rightarrow \text{no solution}$ |
| For $1 \leq x/y < 2$: | |
| $0 < p < x/y$ | $g = -\log m/\kappa(x/y - 1), c^2 = \mathcal{O} \left(m^{x^2/2-1} / \sqrt{-\log m} \right) \rightarrow 0 \Rightarrow \text{RS solution}$ |
| $x/y \leq p < 2x/y - 1$ | $g = -\log m/\kappa(x/y - 1), f(1) = 1, c^2 = \mathcal{O}(m^{f(p)-1}) \rightarrow 0 \Rightarrow \text{RS solution}$ |
| (3) $p = 2x/y - 1$ | $g = -\log m/2\kappa(x/y - 1), c^2 = \frac{1}{2}, x = \frac{y^2 + 2}{2y}$ |
| (4) $2x/y - 1 < p < 2x/y$ | $g = -\log m, c = 1, x = \frac{p^2 y^2 + 2}{2py}$ |
| $p = 2x/y$ | $g = -\log 2m, c = 1, x = \frac{p^2 y^2 + 2}{2py} = \frac{4x^2 + 2}{4x} \Rightarrow \text{no solution}$ |
| $p > 2x/y$ | $g = -\log m, f(p) = f(p) + 1 \Rightarrow \text{no solution}$ |
| For $x/y \geq 2$: | |
| $0 < p < 2x/y - 2$ | $g = -\log m, f(1) = 1, c^2 = \mathcal{O}(m^{f(2)-1}) \rightarrow 0 \Rightarrow \text{RS solution}$ |
| $p = 2x/y - 2$ | $g = -\log m, f(1) = 1, c^2 = \mathcal{O}(m^{f(2)-1}) \rightarrow 0 \Rightarrow \text{RS solution}$ |
| $2x/y - 2 < p < 2x/y - 1$ | $g = -\log m, f(1) = 1, c^2 = \mathcal{O}(m^{f(p)-1}) \rightarrow 0 \Rightarrow \text{RS solution}$ |
| (5) $p = 2x/y - 1$ | $g = -\log m/2, c^2 = \frac{1}{2}, x = \frac{y^2 + 2}{2y}$ |
| (6) $2x/y - 1 < p < 2x/y$ | $g = -\log m, c = 1, x = \frac{p^2 y^2 + 2}{2py}$ |
| $p = 2x/y$ | $g = -\log 2m, c = 1, x = \frac{p^2 y^2 + 2}{2py} = \frac{4x^2 + 2}{4x} \Rightarrow \text{no solution}$ |
| $p > 2x/y$ | $g = -\log m, f(p) = f(p) + 1 \Rightarrow \text{no solution}$ |

TABLE II. Summary of the solutions of the SP equations for m and q_1 . Numbers (1) to (6) denote the cases in which a non-RS solution exists.

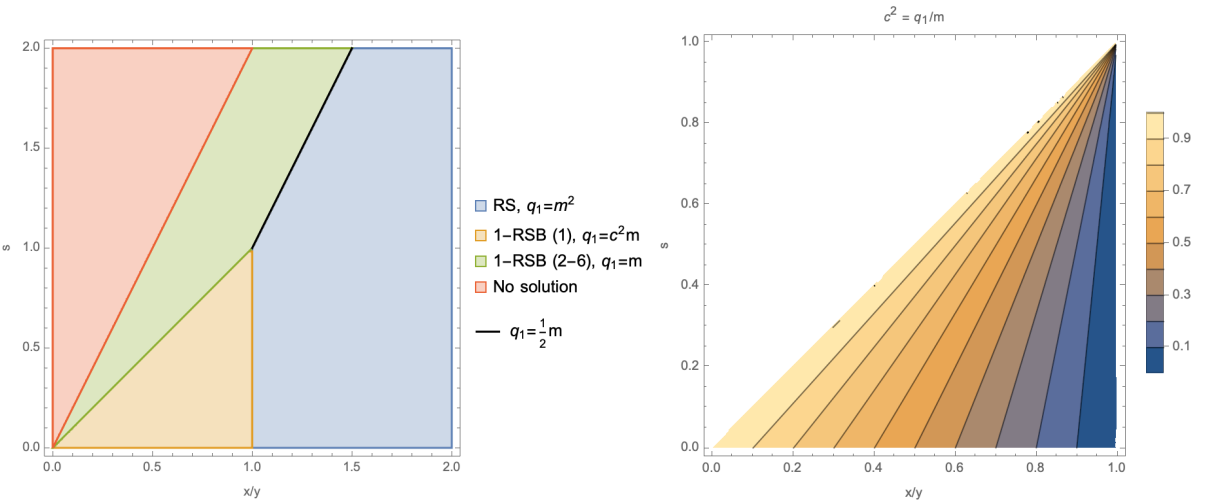


FIG. S2. Right: solution type as a function of x/y and s . Notice that exactly at the boundary between the RS and 1-RSB (4, 6) region, there is the 1-RSB (3,5) solution with $c^2 = 1/2$, signaling a discontinuous transition between the two phases. Left: zoom on the 1-RSB (1) solution, where $0 < c^2 < 1$. We see that $c^2 = K_2/K_1$ interpolates between $c^2 = 0$ for $x/y = 1$ at the boundary with the RS phase, and $c^2 = 1$ for $s = x/y$ at the boundary with the $c^2 = 1$ 1-RSB phase. Notice that the level sets of the equation $c^2 = K_2/K_1$ seem to satisfy $s = 1 + 1/c^2(x/y - 1)$.

- For $2x/y - 1 < p < 2x/y$ and $x/y \geq 1$, the $\ell = 0$ integral equals $1 + m^{\min(f(p), f(1))}$ with $\min(f(p), f(1)) \geq 1$.
- For $p = 2x/y - 1$ and $x/y \geq 2$, the $\ell = 0$ integral equals again $1 + m^{\min(f(p), f(1))}$ with $\min(f(p), f(1)) \geq 1$.

Thus, this term is subleading w.r.t. the first contribution to the complexity in all solution branches, and can be discarded.

We now study

$$\int Dv (1 + e^{\beta H})^p \log1pexp(\beta H). \quad (\text{S59})$$

First of all, we notice that

$$\log1pexp(x) = \log(1 + e^x) = \max(x, 0) + \log\left(1 + e^{-|x|}\right) = \max(x, 0) + \sum_{n \geq 1} d_n e^{-n|x|} \quad (\text{S60})$$

which is a uniformly convergent expansion for $e^{-|x|} < 1$, i.e. $x \neq 0$, and $d_n = (-1)^n/n$ are the coefficient of the expansion of the logarithmic power series. Thus, we have three contributions: one for $v < v_*$, the second coming from the $v > v_*$ power series part and the third coming from $v > v_* \max(0, x)$ part (recall $v_* = x\sqrt{g} > 0$). The first contribution reads

$$\begin{aligned} \int_{-\infty}^{v_*} Dv (1 + e^{\beta H})^p \log1pexp(\beta H) &= \int_{-\infty}^{v_*} Dv \left[\sum_{n \geq 0} \binom{p}{n} e^{n\beta H} \right] \left[\sum_{n \geq 1} d_n e^{n\beta H} \right] \\ &= \int_{-\infty}^{v_*} Dv \sum_{n \geq 1} \left[\sum_{r=1}^n \binom{p}{r} d_r \right] e^{n\beta H} = \sum_{n \geq 1} h_n e^{-nyxg} \int_{-\infty}^{v_*} Dv e^{ny\sqrt{g}v} \\ &= \sum_{n \geq 1} h_n e^{-f(n)g} G((x - ny)\sqrt{g}). \end{aligned} \quad (\text{S61})$$

Now notice that if $0 < x/y < 1$, all terms in the sum contribute to order $\exp(-gx^2/2)/\sqrt{g} \geq \mathcal{O}(m)$ — here we used Table II cases (1, 2) — and are subleading w.r.t. the complexity scaling $m \log 1/m$. If instead $x/y \geq 1$, the $n = 1$ term dominates. In all the relevant solution branches — namely Table II cases (3, 4, 5, 6) — we have $1 = f(p) \leq f(1)$, so that again this term is subleading w.r.t. the complexity scaling $m \log 1/m$. The second contribution reads

$$\begin{aligned} \int_{v_*}^{+\infty} Dv (1 + e^{\beta H})^p \log1pexp(\beta H) &= \int_{v_*}^{+\infty} Dv e^{p\beta H} \left[\sum_{n \geq 0} \binom{p}{n} e^{-n\beta H} \right] \left[\sum_{n \geq 1} d_n e^{-n\beta H} \right] \\ &= \int_{v_*}^{+\infty} Dv e^{p\beta H} \sum_{n \geq 1} \left[\sum_{r=1}^n \binom{p}{r} d_r \right] e^{-n\beta H} = \sum_{n \geq 1} h_n e^{-(p-n)yxg} \int_{v_*}^{+\infty} Dv e^{(p-n)y\sqrt{g}v} \\ &= \sum_{n \geq 1} h_n e^{-f(p-n)g} G(((p-n)y - x)\sqrt{g}). \end{aligned} \quad (\text{S62})$$

In this case, we have that all terms $1 \leq n \leq \lfloor p - x/y \rfloor$ have positive argument in the G function. If $0 < p < x/y + 1$ all terms in the sum contribute to order $\exp(-gx^2/2)/\sqrt{g} \geq \mathcal{O}(m)$ — here we used Table II cases (1, 2, 3, 4) — and are subleading w.r.t. the complexity scaling $m \log 1/m$. If $p \geq x/y + 1$ the leading term is the $n = 1$ one with order $\exp(-gf(p-1))$, but $f(p-1) \geq f(p) = 1$ — here we used Table II cases (3, 4, 5, 6) — and is again subleading w.r.t. the complexity scaling $m \log 1/m$. Thus, the contributions coming from the power series part of the $\log1pexp$ expansion do not contribute at leading order. We now need to study

$$\begin{aligned} \int_{v_*}^{+\infty} Dv \beta H (1 + e^{\beta H})^p &= -xyg \int_{v_*}^{+\infty} Dv (1 + e^{\beta H})^p + y\sqrt{g} \int_{v_*}^{+\infty} Dv v (1 + e^{\beta H})^p \\ &= -xyg \int_{v_*}^{+\infty} Dv (1 + e^{\beta H})^p + y\sqrt{g} \frac{e^{-\frac{1}{2}x^2g}}{\sqrt{2\pi}} + sy^2g \int_{v_*}^{+\infty} Dv (1 + e^{\beta H})^{p-1} e^{\beta H} \\ &\sim -xyg \int_{v_*}^{+\infty} Dv (1 + e^{\beta H})^p + py^2g \int_{v_*}^{+\infty} Dv (1 + e^{\beta H})^{p-1} e^{\beta H} + y\sqrt{g} \frac{e^{-\frac{1}{2}x^2g}}{\sqrt{2\pi}} \\ &= g \sum_{n \geq 0} \left[py^2 \binom{p-1}{n} - xy \binom{p}{n} \right] e^{-f(p-n)g} G(\sqrt{g}((p-n)y - x)) + y\sqrt{g} \frac{e^{-\frac{1}{2}x^2g}}{\sqrt{2\pi}} \end{aligned} \quad (\text{S63})$$

where we integrated by parts and used (S43). Starting from the sum term, we have that all terms $0 \leq n \leq \lfloor p - x/y \rfloor$ have positive argument in the G function. If $0 < p < x/y$ all terms in the sum contribute to the complexity's leading order $g \exp(-gx^2/2)/\sqrt{g} = \mathcal{O}(m \log 1/m)$ — here we used Table II cases (1) — so that

$$\int Dv (1 + e^{\beta H})^p \log 1p \exp(\beta H) = \gamma K_3 m \log \frac{1}{m} + \gamma \frac{y}{\sqrt{2\pi}} m \sqrt{\log \frac{1}{m}} + \mathcal{O}(m) \quad (\text{S64})$$

with

$$K_3 = \frac{1}{\sqrt{2\pi}} \left[py^2 \frac{{}_2F_1 \left(1-p, \frac{x}{y} - p; -p + \frac{x}{y} + 1; -1 \right)}{x - py} - xy \frac{{}_2F_1 \left(-p, \frac{x}{y} - p; -p + \frac{x}{y} + 1; -1 \right)}{x - py} \right]. \quad (\text{S65})$$

If $p \geq x/y$ the leading term is the $n = 0$ one with order $\exp(-gf(p)) = \mathcal{O}(m)$ — here we used Table II cases (2, 3, 4, 5, 6). Moreover, the boundary term is subleading with respect to the tail sum, and the first discarded term is $n = 1$ of order $\mathcal{O}(m^{f(p-1)}) \ll \mathcal{O}(m)$ so that

$$\int Dv (1 + e^{\beta H})^p \log 1p \exp(\beta H) = [py^2 - xy] m \log \frac{1}{m} + \mathcal{O}(m). \quad (\text{S66})$$

Thus, we can sum up our solutions as

- for $0 < p < x/y < 1$,

$$\Sigma(b, p) = \left[\frac{1}{4} p^2 b^2 c^4 - p \gamma K_3 \right] m \log \frac{1}{m} \quad (\text{S67})$$

and $g = -\log \left(m \sqrt{\log \frac{1}{m}} \right)$, $x = \sqrt{2}$, $\gamma K_1 = 1$, $\gamma K_2 = c^2$.

- For $2x/y - 1 < p < 2x/y$ and $x/y \geq 1$,

$$\Sigma(b, p) = \left[1 - \frac{1}{4} p^2 b^2 \right] m \log \frac{1}{m} \quad (\text{S68})$$

and $g = -\log m$, $c = 1$, $\mu = \frac{p^2 b^2 + 2}{2pb}$, under the conditions

$$\left(0 < b \leq \sqrt{2} \text{ and } p > \frac{2}{b^2} \right) \text{ or } \left(b > \sqrt{2} \text{ and } p \geq 1 + \sqrt{\frac{b^2 - 2}{b^2}} \right). \quad (\text{S69})$$

- For $p = 2x/y - 1$ and $x/y \geq 1$,

$$\Sigma(b, p = 4/b^2) = \left[1 - \frac{b^2}{4} \right] m \log \frac{1}{m} \quad (\text{S70})$$

and $g = -\log m$, $c^2 = 1/2$, $\mu = \frac{b^2 + 2}{2b}$, $p = 4/b^2$ under the condition $0 < b \leq 2$. This solution has positive complexity evaluated at the corresponding value of p .

E. Stability in the scaling limit

The condition for the stability of the 1RSB is (see Section I 0 d)

$$\beta^2 \left[\langle \langle \ell(u, v)^4 \rangle_v \rangle_u - 2 \langle \langle \ell(u, v)^3 \rangle_v \rangle_u + \langle \langle \ell(u, v)^2 \rangle_v \rangle_u \right] < 1, \quad (\text{S71})$$

with $\ell(u, v) = \text{logistic}(\beta H(u, v))$, that in the scaling limit reads

$$b^2 \frac{1}{m} \log \frac{1}{m} \int Dv (1 + e^{\beta H})^p [\ell(\beta H)^4 - 2\ell(\beta H)^3 + \ell(\beta H)^2] < 1 \quad (\text{S72})$$

where all denominators and subleading terms in the scaling of β were discarded at leading order. We have two main cases.

a. *Solution (4,6)* For $2x/y - 1 < p < 2x/y$ and $x/y \geq 1$ we have that the leading order of the 3 integral equals $m^{f(p)} = m$, and it cancels. We need to investigate the subleading order. It suffices to show that at the first non-vanishing order of the integral goes to zero fast enough to counterbalance the scaling term $\log(1/m)/m$. But all integrals are of the form (modulo logarithmic terms) $m + m^{1+\epsilon}$ for some strictly positive constants ϵ , so that at the first order with no cancellations we have

$$b^2 \frac{1}{m} \log \frac{1}{m} \times \text{const } m^{1+\epsilon} \sim m^\epsilon \log \frac{1}{m} \rightarrow \infty. \quad (\text{S73})$$

Thus, this 1RSB phase is stable.

b. *Solution (1)* For this solution, we have that in all cases $\ell = 2, 3, 4$ the leading term comes from the resummation. It is equals

$$\gamma (K_4 - 2K_3 + K_2) m \quad (\text{S74})$$

where

$$K_\ell = \frac{1}{\sqrt{2\pi}} \left[\frac{{}_2F_1 \left(\ell - s, \frac{x}{y} - s; -s + \frac{x}{y} + 1; -1 \right)}{x - sy} - \frac{{}_2F_1 \left(\ell - s, \ell - \frac{x}{y}; \ell + 1 - \frac{x}{y}; -1 \right)}{x - \ell y} \right]. \quad (\text{S75})$$

So we have

$$b^2 \log \frac{1}{m} \gamma (K_4 - 2K_3 + K_2) < 1 \quad (\text{S76})$$

which can only be true if $K_4 - 2K_3 + K_2 < 0$ in the $m \rightarrow 0$ limit. Numerically we see that this may be the case only on lines in the phase space, not full $2d$ regions, so that in general this solution is unstable.

IV. THE NON-SYMMETRIC MODEL

In this section we show that the symmetric and non-symmetric models have very similar behavior. We do this by computing explicitly the free entropy in the RS ansatz, and showing that the resulting extremization conditions are the same. Notice that from the structure of the RS computation is natural to infer that the extremisation conditions will be the same to all steps of RSB.

A. The model

We can study the non symmetric model by considering the Hamiltonian

$$E(\sigma, \tau) = \frac{1}{\sqrt{N}} \sum_{i,j} J_{ij} \sigma_i \tau_j \quad (\text{S77})$$

and the measure

$$p(\sigma, \tau) = \frac{1}{Z_J} \exp(\beta H_J + \beta h_\sigma \sum_i \sigma_i + \beta h_\tau \sum_i \tau_i) \quad (\text{S78})$$

where both h 's are chosen such that $\mathbb{E}\langle \sum_i \sigma_i \rangle = \mathbb{E}\langle \sum_i \tau_i \rangle = mN$ — the more general rectangular submatrix problem can be solved similarly by allowing for different values of m . As in the symmetric case, the Boolean vectors σ and τ encode respectively the row-set and column-set of a submatrix of J .

B. Disorder average

The replica computation gives (remember that $\sigma^2 = \sigma$ as $\sigma = 0, 1$ and similar for τ)

$$\begin{aligned}
\mathbb{E}_J Z^n &= \text{Tr}_{\sigma, \tau} \exp \left[\beta h_\sigma \sum_{i,a} \sigma_i^a + \beta h_\tau \sum_{i,a} \tau_i^a \right] \prod_{i,j=1}^N \int D J_{ij} \exp \left[\frac{\beta}{\sqrt{N}} J_{ij} \sum_a \sigma_i^a \tau_j^a \right] \\
&= \text{Tr}_{\sigma, \tau} \exp \left[\beta h_\sigma \sum_{a,i} \sigma_i^a + \beta h_\tau \sum_{a,i} \tau_i^a + \frac{\beta^2}{2N} \sum_{a,b} \left(\sum_i \sigma_i^a \sigma_i^b \right) \left(\sum_i \tau_i^a \tau_i^b \right) \right] \\
&= \text{Tr}_{\sigma, \tau} \exp \left[\beta h_\sigma \sum_{a,i} \sigma_i^a + \beta h_\tau \sum_{a,i} \tau_i^a + \frac{\beta^2}{2N} \sum_a \left(\sum_i \sigma_i^a \right) \left(\sum_i \tau_i^a \right) + \frac{\beta^2}{N} \sum_{a < b} \left(\sum_i \sigma_i^a \sigma_i^b \right) \left(\sum_i \tau_i^a \tau_i^b \right) \right]
\end{aligned} \tag{S79}$$

Now we enforce the order parameters using delta functions and their exponential representation

$$\begin{aligned}
\mathbb{E}_J Z^n &= \int \prod_a dm_\sigma^a dm_\tau^a \prod_{a < b} dq_\sigma^{ab} dq_\tau^{ab} \times \\
&\quad \exp \left[N \beta h_\sigma \sum_a m_\sigma^a + N \beta h_\tau \sum_a m_\tau^a + N \frac{\beta^2}{2} \sum_a m_\sigma^a m_\tau^a + N \beta^2 \sum_{a < b} q_\sigma^{ab} q_\tau^{ab} \right] \times \\
&\quad \int \prod_a d\hat{m}_\sigma^a d\hat{m}_\tau^a \prod_{a < b} d\hat{q}_\sigma^{ab} d\hat{q}_\tau^{ab} \times \\
&\quad \exp \left[-N \sum_a m_\sigma^a \hat{m}_\sigma^a - N \sum_a m_\tau^a \hat{m}_\tau^a - N \sum_{a < b} q_\sigma^{ab} \hat{q}_\sigma^{ab} - N \sum_a q_\tau^{ab} \hat{q}_\tau^{ab} \right] \times \\
&\quad \text{Tr}_{\sigma, \tau} \exp \left[\sum_a \hat{m}_\sigma^a \sum_i \sigma_i^a + \sum_a \hat{m}_\tau^a \sum_i \tau_i^a + \sum_{a < b} \hat{q}_\sigma^{ab} \left(\sum_i \sigma_i^a \sigma_i^b \right) + \sum_{a < b} \hat{q}_\tau^{ab} \left(\sum_i \tau_i^a \tau_i^b \right) \right] \\
&= \int \prod_a dm_\sigma^a dm_\tau^a \prod_{a < b} dq_\sigma^{ab} dq_\tau^{ab} \times \\
&\quad \exp \left[N \beta h_\sigma \sum_a m_\sigma^a + N \beta h_\tau \sum_a m_\tau^a + N \frac{\beta^2}{2} \sum_a m_\sigma^a m_\tau^a + N \beta^2 \sum_{a < b} q_\sigma^{ab} q_\tau^{ab} \right] \times \\
&\quad \int \prod_a d\hat{m}_\sigma^a d\hat{m}_\tau^a \prod_{a < b} d\hat{q}_\sigma^{ab} d\hat{q}_\tau^{ab} \times \\
&\quad \exp \left[-N \sum_a m_\sigma^a \hat{m}_\sigma^a - N \sum_a m_\tau^a \hat{m}_\tau^a - N \sum_{a < b} q_\sigma^{ab} \hat{q}_\sigma^{ab} - N \sum_a q_\tau^{ab} \hat{q}_\tau^{ab} \right] \times \\
&\quad \exp \left[N \log \text{Tr}_\sigma \exp \left(\sum_a \hat{m}_\sigma^a \sigma^a + \sum_{a < b} \hat{q}_\sigma^{ab} \sigma^a \sigma^b \right) + N \log \text{Tr}_\tau \exp \left(\sum_a \hat{m}_\tau^a \tau^a + \sum_{a < b} \hat{q}_\tau^{ab} \tau^a \tau^b \right) \right]
\end{aligned} \tag{S80}$$

C. RS ansatz

The trace terms can be computed as

$$\begin{aligned}
N \log \text{Tr}_\sigma \exp \left(\sum_a \hat{m}_\sigma^a \sigma^a + \sum_{a < b} \hat{q}_\sigma^{ab} \sigma^a \sigma^b \right) &= N \log \text{Tr}_\sigma \exp \left(\hat{m}_\sigma \sum_a \sigma^a + \hat{q}_\sigma \sum_{a < b} \sigma^a \sigma^b \right) \\
&= N \log \text{Tr}_\sigma \exp \left(\hat{m}_\sigma \sum_a \sigma^a + \frac{\hat{q}_\sigma}{2} \sum_{a,b} \sigma^a \sigma^b - \frac{\hat{q}_\sigma}{2} \sum_a \sigma^a \right) \\
&= N \log \text{Tr}_\sigma \exp \left(\left(\hat{m}_\sigma - \frac{\hat{q}_\sigma}{2} \right) \sum_a \sigma^a + \frac{\hat{q}_\sigma}{2} \left(\sum_a \sigma^a \right)^2 \right) \\
&= N \log \int Dz \text{Tr}_\sigma \exp \left(\left(\hat{m}_\sigma - \frac{\hat{q}_\sigma}{2} + z \sqrt{\hat{q}_\sigma} \right) \sum_a \sigma^a \right) \quad (\text{S81}) \\
&= N \log \int Dz \left[\text{Tr}_\sigma \exp \left(\left(\hat{m}_\sigma - \frac{\hat{q}_\sigma}{2} + z \sqrt{\hat{q}_\sigma} \right) \sigma \right) \right]^n \\
&= N \log \int Dz \left[1 + \exp \left(\hat{m}_\sigma - \frac{\hat{q}_\sigma}{2} + z \sqrt{\hat{q}_\sigma} \right) \right]^n \\
&\approx N \log \left[1 + n \int Dz \log1pexp \left(\hat{m}_\sigma - \frac{\hat{q}_\sigma}{2} + z \sqrt{\hat{q}_\sigma} \right) + \dots \right] \\
&\approx Nn \int Dz \log1pexp \left(\hat{m}_\sigma - \frac{\hat{q}_\sigma}{2} + z \sqrt{\hat{q}_\sigma} \right) + \dots
\end{aligned}$$

giving

$$\langle Z^n \rangle_{J, \text{RS}} = \int \prod_a dm_\sigma^a dm_\tau^a d\hat{m}_\sigma^a d\hat{m}_\tau^a \prod_{a < b} dq_\sigma^{ab} dq_\tau^{ab} d\hat{q}_\sigma^{ab} d\hat{q}_\tau^{ab} \exp NnS(\dots) \quad (\text{S82})$$

where

$$\begin{aligned}
S(\dots) &= \beta h_\sigma m_\sigma + \beta h_\tau m_\tau + \frac{\beta^2}{2} m_\sigma m_\tau - \frac{\beta^2}{2} q_\sigma q_\tau - m_\sigma \hat{m}_\sigma - m_\tau \hat{m}_\tau + \frac{1}{2} q_\sigma \hat{q}_\sigma + \frac{1}{2} q_\tau \hat{q}_\tau \\
&+ \int Dz_\sigma \log1pexp \left(\hat{m}_\sigma - \frac{\hat{q}_\sigma}{2} + z_\sigma \sqrt{\hat{q}_\sigma} \right) + \int Dz_\tau \log1pexp \left(\hat{m}_\tau - \frac{\hat{q}_\tau}{2} + z_\tau \sqrt{\hat{q}_\tau} \right) \quad (\text{S83})
\end{aligned}$$

D. RS saddle-point equations

The SP equations in the non-hat variables are

$$\begin{aligned}
\hat{m}_\sigma &= \beta h_\sigma + \frac{\beta^2}{2} m_\tau \\
\hat{m}_\tau &= \beta h_\tau + \frac{\beta^2}{2} m_\sigma \\
\hat{q}_\sigma &= \beta^2 q_\tau \\
\hat{q}_\tau &= \beta^2 q_\sigma
\end{aligned} \quad (\text{S84})$$

and the others are (already with the substitutions allowed by the previous equations)

$$\begin{aligned}
m_\sigma &= \int Dz_\sigma \text{logistic} \left(\hat{m}_\sigma - \frac{\hat{q}_\sigma}{2} + z_\sigma \sqrt{\hat{q}_\sigma} \right) = \int Dz_\sigma \text{logistic} \beta H_\sigma \\
q_\sigma &= -2 \int Dz_\sigma \text{logistic} \left(\hat{m}_\sigma - \frac{\hat{q}_\sigma}{2} + z_\sigma \sqrt{\hat{q}_\sigma} \right) \left(-\frac{1}{2} + \frac{z}{2\sqrt{\hat{q}_\sigma}} \right) \\
&= \int Dz_\sigma \left(1 - \frac{z}{\sqrt{\hat{q}_\sigma}} \right) \text{logistic} \left(\hat{m}_\sigma - \frac{\hat{q}_\sigma}{2} + z_\sigma \sqrt{\hat{q}_\sigma} \right) \\
&= m_\sigma - \frac{1}{\sqrt{\hat{q}_\sigma}} \int Dz_\sigma z_\sigma \text{logistic} \left(\hat{m}_\sigma - \frac{\hat{q}_\sigma}{2} + z_\sigma \sqrt{\hat{q}_\sigma} \right) \\
&= m_\sigma - \frac{1}{\sqrt{\hat{q}_\sigma}} \int Dz_\sigma \partial_{z_\sigma} \text{logistic} \left(\hat{m}_\sigma - \frac{\hat{q}_\sigma}{2} + z_\sigma \sqrt{\hat{q}_\sigma} \right) \\
&= m_\sigma - \int Dz_\sigma (1 - \text{logistic} \beta H_\sigma) \text{logistic} \beta H_\sigma \\
&= \int Dz_\sigma (\text{logistic} \beta H_\sigma)^2
\end{aligned} \tag{S85}$$

where

$$H_\sigma = h_\sigma + \frac{\beta}{2} (m_\tau - q_\tau) + z_\sigma \sqrt{q_\tau} \tag{S86}$$

and the same for τ . Notice that we obtain the same type of equations as for the symmetric model, but with a coupling between the two sets of spins.

Notice that a solution of these equations is the symmetric one, meaning $m_\tau = m_\sigma$ and same for h, q , giving

$$\begin{aligned}
m &= \int Dz \text{logistic}(\beta H), \\
q &= \int Dz (\text{logistic}(\beta H))^2,
\end{aligned} \tag{S87}$$

with $H = h + \frac{\beta}{2}(m - q) + z\sqrt{q}$, which are exactly the same equations as in the symmetric version of the problem.

V. DETAILS OF THE TYPE-I STABILITY COMPUTATION

We will use the following notations for the 2-RSB (and analogous for the 1-RSB) saddle-point equations

$$\begin{aligned}
\langle f(u) \rangle_u &= \int Du f(u), \\
\langle f(u, v) \rangle_v &= \frac{1}{N_v(u)} \int Dv f(u, v) N_z(u, v)^{p_1/p_2}, \\
\langle f(u, v, z) \rangle_z &= \frac{1}{N_z(u, v)} \int Dz f(u, v, z) \left(1 + e^{\beta H(u, v, z)} \right)^{p_2}, \\
N_v(u) &= \int Dv N_z(u, v)^{p_1/p_2}, \\
N_z(u, v) &= \int Dz \left(1 + e^{\beta H(u, v, z)} \right)^{p_2},
\end{aligned} \tag{S88}$$

so that the equation for q_2 reads:

$$q_2 = \left\langle \langle \langle \ell^2 \rangle_z \rangle_v \right\rangle_u, \tag{S89}$$

where $\ell = \text{logistic}(\beta H_{2\text{RSB}})$ and

$$H_{2\text{RSB}} \equiv H(u, v, z) = h + \frac{\beta}{2} (m - q_2) + \sqrt{q_0} u + \sqrt{q_1 - q_0} v + \sqrt{q_2 - q_1} z \tag{S90}$$

Let

$$\begin{aligned}
m^{2\text{RSB}} &= m, \\
q_2^{2\text{RSB}} &= q_1 + \epsilon, \\
q_1^{2\text{RSB}} &= q_1, \\
q_0^{2\text{RSB}} &= q_0, \\
p_2^{2\text{RSB}} &= x, \\
p_1^{2\text{RSB}} &= p_1,
\end{aligned} \tag{S91}$$

with $\epsilon > 0$ small, $x \in (p_1, 1)$ and m, q_1, q_0, p_1 are the solutions to the 1-RSB SP equations.

We start by expanding

$$\begin{aligned}
\beta H_{2\text{RSB}} &= \beta h + \frac{\beta^2}{2}(m^{2\text{RSB}} - q_2^{2\text{RSB}}) + \beta\sqrt{q_0^{2\text{RSB}}}u + \beta\sqrt{q_1^{2\text{RSB}} - q_0^{2\text{RSB}}}v + \beta\sqrt{q_2^{2\text{RSB}} - q_1^{2\text{RSB}}}z \\
&= \beta h + \frac{\beta^2}{2}(m - q_1 - \epsilon) + \beta\sqrt{q_0}u + \beta\sqrt{q_1 - q_0}v + \beta\sqrt{\epsilon}z \\
&= \beta H_{1\text{RSB}}(u, v) + \beta\sqrt{\epsilon}z - \frac{\beta^2}{2}\epsilon
\end{aligned} \tag{S92}$$

so that $(\ell(u, v) = \ell(\beta H_{1\text{RSB}}(u, v))$ is the logistic function)

$$\begin{aligned}
(1 + e^{\beta H_{2\text{RSB}}})^{p_2^{2\text{RSB}}} &= \left(1 + e^{\beta H_{1\text{RSB}}(u, v) + \beta\sqrt{\epsilon}z - \frac{\beta^2}{2}\epsilon}\right)^x \\
&= \left(1 + e^{\beta H_{1\text{RSB}}(u, v)}\right)^x \left(1 + \ell(u, v) \left(e^{\beta\sqrt{\epsilon}z - \frac{\beta^2}{2}\epsilon} - 1\right)\right)^x \\
&= \left(1 + e^{\beta H_{1\text{RSB}}(u, v)}\right)^x \left(1 + \ell(u, v) \left(\beta\sqrt{\epsilon}z + (z^2 - 1)\frac{\beta^2}{2}\epsilon + \mathcal{O}(\epsilon^{3/2})\right)\right)^x \\
&= \left(1 + e^{\beta H_{1\text{RSB}}(u, v)}\right)^x \left(1 + x\ell(u, v) \left(\beta\sqrt{\epsilon}z + (z^2 - 1)\frac{\beta^2}{2}\epsilon\right) + \frac{x(x-1)}{2}\beta^2\epsilon z^2\ell(u, v)^2 + \mathcal{O}(\epsilon^{3/2})\right) \\
&= \left(1 + e^{\beta H_{1\text{RSB}}(u, v)}\right)^x \left(1 + \sqrt{\epsilon}z\beta x\ell(u, v) + \epsilon\frac{\beta^2}{2}x\ell(u, v) \left(z^2 - 1 + (x-1)z^2\ell(u, v)\right) + \mathcal{O}(\epsilon^{3/2})\right)
\end{aligned} \tag{S93}$$

implying

$$\begin{aligned}
N_z^{2\text{RSB}}(u, v) &= \int Dz \left(1 + e^{\beta H_{1\text{RSB}}(u, v)}\right)^x \left(1 + \sqrt{\epsilon}z\beta x\ell(u, v) + \epsilon\frac{\beta^2}{2}x\ell(u, v) \left(z^2 - 1 + (x-1)z^2\ell(u, v)\right) + \mathcal{O}(\epsilon^{3/2})\right) \\
&= \left(1 + e^{\beta H_{1\text{RSB}}(u, v)}\right)^x \left(1 + \epsilon\frac{\beta^2}{2}x(x-1)\ell(u, v)^2 + \mathcal{O}(\epsilon^2)\right).
\end{aligned} \tag{S94}$$

Moreover

$$\begin{aligned}
&\ell \left(\beta H_{1\text{RSB}}(u, v) + \beta\sqrt{\epsilon}z - \frac{\beta^2}{2}\epsilon \right) \\
&= \ell(u, v) \left(1 + \sqrt{\epsilon}z\beta(1 - \ell(u, v)) - \epsilon\frac{\beta^2}{2}(1 - \ell(u, v)) \left[1 - z^2 + 2z^2\ell(u, v)\right] + \mathcal{O}(\epsilon^{3/2}) \right)
\end{aligned} \tag{S95}$$

and

$$\begin{aligned}
&\ell \left(\beta H_{1\text{RSB}}(u, v) + \beta\sqrt{\epsilon}z - \frac{\beta^2}{2}\epsilon \right)^2 \\
&= \ell(u, v)^2 \left(1 + \sqrt{\epsilon}z\beta(1 - \ell(u, v)) - \epsilon\frac{\beta^2}{2}(1 - \ell(u, v)) \left[1 - z^2 + 2z^2\ell(u, v)\right] + \mathcal{O}(\epsilon^{3/2}) \right)^2 \\
&= \ell(u, v)^2 \left(1 + 2\sqrt{\epsilon}z\beta(1 - \ell(u, v)) + \epsilon z^2\beta^2(1 - \ell(u, v))^2 - \epsilon\beta^2(1 - \ell(u, v)) \left[1 - z^2 + 2z^2\ell(u, v)\right] + \mathcal{O}(\epsilon^{3/2}) \right) \\
&= \ell(u, v)^2 \left(1 + 2\sqrt{\epsilon}z\beta(1 - \ell(u, v)) - \epsilon\beta^2(1 - \ell(u, v)) \left[1 - 2z^2 + 3z^2\ell(u, v)\right] + \mathcal{O}(\epsilon^{3/2}) \right)
\end{aligned} \tag{S96}$$

Thus, we have that

$$\begin{aligned}
\langle \ell(u, v, z)^2 \rangle_z^{2\text{RSB}} &= \left(1 + e^{\beta H_{1\text{RSB}}(u, v)}\right)^{-x} \left(1 - \epsilon \frac{\beta^2}{2} x(x-1) \ell(u, v)^2 + \mathcal{O}(\epsilon^2)\right) \times \\
&\times \int Dz \left(1 + e^{\beta H_{1\text{RSB}}(u, v)}\right)^x \left(1 + \sqrt{\epsilon} z \beta x \ell(u, v) + \epsilon \frac{\beta^2}{2} x \ell(u, v) (z^2 - 1 + (x-1)z^2 \ell(u, v)) + \mathcal{O}(\epsilon^{3/2})\right) \times \\
&\times \ell(u, v)^2 \left(1 + 2\sqrt{\epsilon} z \beta (1 - \ell(u, v)) - \epsilon \beta^2 (1 - \ell(u, v)) [1 - 2z^2 + 3z^2 \ell(u, v)] + \mathcal{O}(\epsilon^{3/2})\right) \\
&= \ell(u, v)^2 \left(1 - \epsilon \frac{\beta^2}{2} x(x-1) \ell(u, v)^2 + \mathcal{O}(\epsilon^2)\right) \int Dz \left(1 + \sqrt{\epsilon} z \beta x \ell(u, v) + 2\sqrt{\epsilon} z \beta (1 - \ell(u, v))\right. \\
&\left.+ 2\epsilon z^2 \beta^2 x \ell(u, v) (1 - \ell(u, v)) + \epsilon \frac{\beta^2}{2} x \ell(u, v) (z^2 - 1 + (x-1)z^2 \ell(u, v)) - \epsilon \beta^2 (1 - \ell(u, v)) [1 - 2z^2 + 3z^2 \ell(u, v)]\right. \\
&\left.+ \mathcal{O}(\epsilon^{3/2})\right) \\
&= \ell(u, v)^2 \left(1 - \epsilon \frac{\beta^2}{2} x(x-1) \ell(u, v)^2 + \mathcal{O}(\epsilon^2)\right) \times \\
&\times \left(1 + 2\epsilon \beta^2 x \ell(u, v) (1 - \ell(u, v)) + \epsilon \frac{\beta^2}{2} x(x-1) \ell(u, v)^2 - \epsilon \beta^2 (1 - \ell(u, v)) (3\ell(u, v) - 1) + \mathcal{O}(\epsilon^2)\right) \\
&= \ell(u, v)^2 (1 + 2\epsilon \beta^2 x \ell(u, v) (1 - \ell(u, v)) - \epsilon \beta^2 (1 - \ell(u, v)) (3\ell(u, v) - 1) + \mathcal{O}(\epsilon^2))
\end{aligned} \tag{S97}$$

Now

$$\begin{aligned}
N_z^{2\text{RSB}}(u, v)^{p_1^{2\text{RSB}}/p_2^{2\text{RSB}}} &= N_z^{2\text{RSB}}(u, v)^{p_1/x} \\
&= \left(1 + e^{\beta H_{1\text{RSB}}(u, v)}\right)^{p_1} \left(1 + \epsilon \frac{\beta^2}{2} x(x-1) \ell(u, v)^2 + \mathcal{O}(\epsilon^2)\right)^{p_1/x} \\
&= \left(1 + e^{\beta H_{1\text{RSB}}(u, v)}\right)^{p_1} \left(1 + \epsilon \frac{\beta^2}{2} p_1(x-1) \ell(u, v)^2 + \mathcal{O}(\epsilon^2)\right).
\end{aligned} \tag{S98}$$

so that

$$\begin{aligned}
N_v^{2\text{RSB}}(u) &= \int Dv N_z^{2\text{RSB}}(u, v)^{p_1^{2\text{RSB}}/p_2^{2\text{RSB}}} \\
&= \int Dv \left(1 + e^{\beta H_{1\text{RSB}}(u, v)}\right)^{p_1} \left(1 + \epsilon \frac{\beta^2}{2} p_1(x-1) \ell(u, v)^2 + \mathcal{O}(\epsilon^2)\right) \\
&= N_v(u) \left(1 + \epsilon \frac{\beta^2}{2} p_1(x-1) \langle \ell(u, v)^2 \rangle_v + \mathcal{O}(\epsilon^2)\right)
\end{aligned} \tag{S99}$$

and

$$\begin{aligned}
\left\langle \langle \ell(u, v, z)^2 \rangle_z^{2\text{RSB}} \right\rangle_v^{2\text{RSB}} &= N_v(u)^{-1} \left(1 - \epsilon \frac{\beta^2}{2} p_1(x-1) \langle \ell(u, v)^2 \rangle_v + \mathcal{O}(\epsilon^2) \right) \times \\
&\quad \times \int Dv \left(1 + e^{\beta H_{1\text{RSB}}(u, v)} \right)^{p_1} \left(1 + \epsilon \frac{\beta^2}{2} p_1(x-1) \ell(u, v)^2 + \mathcal{O}(\epsilon^2) \right) \times \\
&\quad \times \ell(u, v)^2 (1 + 2\epsilon\beta^2 x \ell(u, v)(1 - \ell(u, v)) - \epsilon\beta^2(1 - \ell(u, v)) (3\ell(u, v) - 1) + \mathcal{O}(\epsilon^2)) \\
&= \left(1 - \epsilon \frac{\beta^2}{2} p_1(x-1) \langle \ell(u, v)^2 \rangle_v + \mathcal{O}(\epsilon^2) \right) \times \\
&\quad \times \left\langle \ell(u, v)^2 \left(1 + \epsilon \frac{\beta^2}{2} p_1(x-1) \ell(u, v)^2 + 2\epsilon\beta^2 x \ell(u, v)(1 - \ell(u, v)) - \epsilon\beta^2(1 - \ell(u, v)) (3\ell(u, v) - 1) + \mathcal{O}(\epsilon^2) \right) \right\rangle_v \\
&= \left(1 - \epsilon \frac{\beta^2}{2} p_1(x-1) \langle \ell(u, v)^2 \rangle_v + \mathcal{O}(\epsilon^2) \right) \times \\
&\quad \times \left\langle \ell(u, v)^2 + \epsilon \frac{\beta^2}{2} p_1(x-1) \ell(u, v)^4 + 2\epsilon\beta^2 x \ell(u, v)^3 (1 - \ell(u, v)) - \epsilon\beta^2(1 - \ell(u, v)) (3\ell(u, v) - 1) \ell(u, v)^2 + \mathcal{O}(\epsilon^2) \right\rangle_v \\
&= \left(1 - \epsilon \frac{\beta^2}{2} p_1(x-1) \langle \ell(u, v)^2 \rangle_v + \mathcal{O}(\epsilon^2) \right) \times \\
&\quad \times \left(\langle \ell(u, v)^2 \rangle_v + \epsilon \frac{\beta^2}{2} p_1(x-1) \langle \ell(u, v)^4 \rangle_v + 2\epsilon\beta^2 x \langle \ell(u, v)^3 \rangle_v - 2\epsilon\beta^2 x \langle \ell(u, v)^4 \rangle_v - 3\epsilon\beta^2 \langle \ell(u, v)^3 \rangle_v \right. \\
&\quad \left. + \epsilon\beta^2 \langle \ell(u, v)^2 \rangle_v + 3\epsilon\beta^2 \langle \ell(u, v)^4 \rangle_v - \epsilon\beta^2 \langle \ell(u, v)^3 \rangle_v + \mathcal{O}(\epsilon^2) \right) \\
&= \left(1 - \epsilon \frac{\beta^2}{2} p_1(x-1) \langle \ell(u, v)^2 \rangle_v + \mathcal{O}(\epsilon^2) \right) \times \\
&\quad \times \left(\langle \ell(u, v)^2 \rangle_v + \epsilon \frac{\beta^2}{2} p_1(x-1) \langle \ell(u, v)^4 \rangle_v + 2\epsilon\beta^2 x \langle \ell(u, v)^3 \rangle_v - 2\epsilon\beta^2 x \langle \ell(u, v)^4 \rangle_v - 3\epsilon\beta^2 \langle \ell(u, v)^3 \rangle_v \right. \\
&\quad \left. + \epsilon\beta^2 \langle \ell(u, v)^2 \rangle_v + 3\epsilon\beta^2 \langle \ell(u, v)^4 \rangle_v - \epsilon\beta^2 \langle \ell(u, v)^3 \rangle_v + \mathcal{O}(\epsilon^2) \right) \\
&= \langle \ell(u, v)^2 \rangle_v + \epsilon \frac{\beta^2}{2} \left[(6 + p_1 x - p_1 - 4x) \langle \ell(u, v)^4 \rangle_v + 4(x-2) \langle \ell(u, v)^3 \rangle_v + 2 \langle \ell(u, v)^2 \rangle_v + p_1(1-x) \langle \ell(u, v)^2 \rangle_v^2 \right] + \mathcal{O}(\epsilon^2)
\end{aligned} \tag{S100}$$

so that the SP equation for q_2 reads

$$\begin{aligned}
q_2 + \epsilon &= \left\langle \left\langle \langle \ell(u, v, z) \rangle_z^{2\text{RSB}} \right\rangle_v^{2\text{RSB}} \right\rangle_u^{2\text{RSB}} \\
&= \langle \langle \ell(u, v)^2 \rangle_v \rangle_u + \epsilon \frac{\beta^2}{2} \left[(6 + p_1 x - p_1 - 4x) \langle \langle \ell(u, v)^4 \rangle_v \rangle_u + 4(x-2) \langle \langle \ell(u, v)^3 \rangle_v \rangle_u \right. \\
&\quad \left. + 2 \langle \langle \ell(u, v)^2 \rangle_v \rangle_u + p_1(1-x) \langle \langle \ell(u, v)^2 \rangle_v \rangle_u^2 \right] + \mathcal{O}(\epsilon^2)
\end{aligned} \tag{S101}$$

The threshold for the linear stability is that the perturbation decreases as the fixed point iterations go on, which happens if

$$\frac{\beta^2}{2} \left[(6 + p_1 x - p_1 - 4x) \langle \langle \ell(u, v)^4 \rangle_v \rangle_u + 4(x-2) \langle \langle \ell(u, v)^3 \rangle_v \rangle_u + 2 \langle \langle \ell(u, v)^2 \rangle_v \rangle_u + p_1(1-x) \langle \langle \ell(u, v)^2 \rangle_v \rangle_u^2 \right] < 1 \tag{S102}$$

Notice that this condition depends on x . Isolating x we obtain

$$\begin{aligned}
&(6 - p_1) \langle \langle \ell(u, v)^4 \rangle_v \rangle_u - 8 \langle \langle \ell(u, v)^3 \rangle_v \rangle_u + 2 \langle \langle \ell(u, v)^2 \rangle_v \rangle_u + p_1 \langle \langle \ell(u, v)^2 \rangle_v \rangle_u^2 \\
&+ x \left[p_1 \left(\langle \langle \ell(u, v)^4 \rangle_v \rangle_u - \langle \langle \ell(u, v)^2 \rangle_v \rangle_u^2 \right) + 4 \left(\langle \langle \ell(u, v)^3 \rangle_v \rangle_u - \langle \langle \ell(u, v)^4 \rangle_v \rangle_u \right) \right] < \frac{2}{\beta^2}.
\end{aligned} \tag{S103}$$

The most stringent stability condition is given by $x = 1$, giving

$$\beta^2 \left[\langle \langle \ell(u, v)^4 \rangle_v \rangle_u - 2 \langle \langle \ell(u, v)^3 \rangle_v \rangle_u + \langle \langle \ell(u, v)^2 \rangle_v \rangle_u \right] < 1. \tag{S104}$$